PLOS ONE

RESEARCH ARTICLE

Solvent based fractional biosynthesis, phytochemical analysis, and biological activity of silver nanoparticles obtained from the extract of *Salvia moorcroftiana*

Maham Khan[1], Tariq Khan[1]*, Shahid Wahab[2,3], Muhammad Aasim[1], Tauqir A. Sherazi[4¤], Muhammad Zahoor[5], Soon-Il Yun[2,3]

1 Department of Biotechnology, University of Malakand, Khyber Pakhtunkhwa, Pakistan, **2** Department of Food Science and Technology, College of Agriculture and Life Sciences, Jeonbuk National University, Jeonju, Republic of South Korea, **3** Department of Agricultural Convergence Technology, College of Agriculture and Life Science, Jeonbuk National University, Jeonju, Republic of South Korea, **4** Department of Chemistry, COMSATS University Islamabad, Abbottabad Campus, Abbottabad, Pakistan, **5** Department of Biochemistry, University of Malakand, Khyber Pakhtunkhwa, Pakistan

¤ Current address: INM—Leibniz Institute for New Materials, Saarbrücken, Germany
* tariqkhan@uom.edu.pk

Check for updates

OPEN ACCESS

Citation: Khan M, Khan T, Wahab S, Aasim M, Sherazi TA, Zahoor M, et al. (2023) Solvent based fractional biosynthesis, phytochemical analysis, and biological activity of silver nanoparticles obtained from the extract of *Salvia moorcroftiana*. PLoS ONE 18(10): e0287080. https://doi.org/10.1371/journal.pone.0287080

Editor: Thanh-Danh Nguyen, Vietnam Academy of Science and Technology, VIET NAM

Received: May 28, 2023

Accepted: September 27, 2023

Published: October 26, 2023

Copyright: © 2023 Khan et al. This is an open access article distributed under the terms of the Creative Commons Attribution License, which permits unrestricted use, distribution, and reproduction in any medium, provided the original author and source are credited.

Data Availability Statement: All relevant data are within the paper.

Funding: This work is partially funded by the project awarded by the international foundation for science and partially by the Department of Biotechnology, University of Malakand, Pakistan. The funders had no role in study design, data collection and analysis, decision to publish, or preparation of the manuscript.

Abstract

Multi-drug resistant bacteria sometimes known as "superbugs" developed through overuse and misuse of antibiotics are determined to be sensitive to small concentrations of silver nanoparticles. Various methods and sources are under investigation for the safe and efficient synthesis of silver nanoparticles having effective antibacterial activity even at low concentrations. We used a medicinal plant named *Salvia moorcroftiana* to extract phytochemicals with antibacterial, antioxidant, and reducing properties. Three types of solvents; from polar to nonpolar, i.e., water, dimethyl sulfoxide (DMSO), and hexane, were used to extract the plant as a whole and as well as in fractions. The biosynthesized silver nanoparticles in all extracts (except hexane-based extract) were spherical, smaller than 20 nm, polydispersed (PDI ranging between 0.2 and 0.5), and stable with repulsive force of action (average zeta value = -18.55±1.17). The tested bacterial strains i.e., *Klebsiella pneumoniae*, *Pseudomonas aeruginosa*, *Staphylococcus aureus*, *and Enterococcus faecalis* were found to be sensitive to even small concentrations of Ag-NPs, especially *P. aeruginosa*. The antibacterial effect of these Ag-NPs was associated with their ability to generate reactive oxygen species. DMSO (in fraction) could efficiently extract antibacterial phytochemicals and showed activity against MDR bacteria (inhibition zone = 11–12 mm). Thus, the antibacterial activity of fractionated DMSO extract was comparable to that of Ag-NPs because it contained phytochemicals having solid antibacterial potential. Furthermore, Ag-NPs synthesized from this extract owned superior antibacterial activity. However, whole aqueous extract-based Ag-NPs MIC was least (7–32 μg/mL) as compared to others.

Competing interests: The authors have declared that no competing interests exist.

1. Introduction

Since the discovery of penicillin, the population across the globe has relied on antibiotics to fight microbial infections. Regrettably, microbes have found a way to resist the action of antibiotics that were once effective due to their misuse, combined use, and over-prescription [1]. The development of multi-drug resistant microbes has now become a universal threat with severe results in administering infectious illnesses caused by pathogens [2]. The need to overcome this problem has been well-recognized and highly investigated. Researchers are coming up with solutions to combat antibiotic resistance, among which nanotechnology is leading the race. Nanoparticles have emerged as unique particles with size-dependent physicochemical characteristics that are proven to have antibacterial potential [3]. Silver nanoparticles (Ag-NPs) have attracted attention as they hold great promise in combating the challenge of antimicrobial resistance due to their extraordinary, broad-spectrum, and strong antimicrobial properties [4]. The antibacterial mechanism of Ag-NPs has been extensively studied. In various studies, the mechanism of action of Ag-NPs is revealed to change the structure of bacterial cell wall, increase the permeability of cell membranes, and plasmolysis, inhibit respiration, suppress DNA replication, change the intracellular ATP levels, generate ROS, and disrupt cell integrity. All the ways through which Ag-NPs interact with bacteria are very effective, and the bacteria cannot easily develop resistance to them as compared to antibiotics because, for that, bacteria would have to target multiple mechanisms of action [5]. A study reported the potency of Ag+ in Ag-NPs to generate ROS at molecular levels that induce oxidative stress at the cellular level leading to increased levels of calcium in intracellular space, disruption of membranes, phosphatidylserine exposure in the outer membrane, DNA degradation and activation of caspase-like protein [6]. A recent study by Buszewski, Rogowska [7] observed a similar inhibitory effect on the growth of *S. aureus* and *P. aeruginosa* when treated with bioactive Ag-NPs. Several important steps occur when Ag-NPs penetrate the cell membranes of bacteria. The silver ions alter the DNA's replication process and cause it to cease replicating, leading to cell death [8]. Ag-NPs can manage antibiotic resistance because no microbial resistance against Ag+ or Ag-NPs has been observed [9].

For the efficient synthesis of nanoparticles, green methods employing microbial cells, plant extract, and natural polymers have been developed. These methods are cost-effective, environment-friendly, and energy-saving [10–12]. Among the available biosynthetic methods, the synthesis of nanoparticles using plant extract is the most favorable. Ag-NPs can be synthesized by mixing silver nitrate (metal salt) and plant extract in a proper ratio. Phytochemicals reduce silver ions and stabilize them by capping, resulting in stable Ag-NPs with possibly less toxicity. Various plants have been employed to synthesize Ag-NPs with little or no variation in the process. *Conocarpus lancifolius* leaf extract [13], *Phoenix dactylifera* [14], *Santalum album* leaf extract [15], Mulberry leaves extract, and *Amaranthus cruentus* [16] are some of the recent examples of plants employed for the synthesis of Ag-NPs with antibacterial applications.

Synthesis of Ag-NPs using plant extract is a safe and green method that can be easily scaled up for producing a large amount of nanoparticles [17]. Plant metabolites actively participate in the synthesis of nanoparticles by reducing and capping metallic cations. These phytochemicals are known to possess good antimicrobial potential and have been attributed to the increased antimicrobial effect of nanoparticles capped by them in the process of biological synthesis through plant extracts. Alkaloids, acetylenes, coumarins, flavonoids and isoflavonoids, iridoids, lignans, macrolides, phenolics (other than flavonoids and lignans), polypeptides, quinones, steroidal saponins, terpenoids, and xanthones have been identified to possess strong effect against resistant bacteria (Saleem et al 2010). Bearing in mind the antibacterial properties

of these compounds, which have been used for centuries, are a source of new therapeutic agents.

The extraction of phytochemicals depends on the type of extraction technique and nature of the solvent because the different polarity and chemical characteristics may or may not allow the dissolution of phytochemicals in particular solvents. Thus, various solvents have different affinity for phytochemicals from plants [18]. Phenolic acids, flavonoids, tannins, alkaloids, etc., can be extracted in polar or less polar solvents [19]. In comparison, components of essential oils and tocopherol can be obtained through extraction in nonpolar solvents [20]. Thus, solvent-based plant extracts can help us to reach the specific group of plant compounds that is responsible for the synthesis of nanoparticles with high bactericidal activity, stability, and dispersity.

Salvia moorcroftiana, commonly known as "kallijari" in Pakistan is a herbaceous plant known to have medicinal properties to relieve pain, fever, and inflammation [21]. The plant contains valuable phytochemical contents like essential oils, flavonoids and polyphenols, tannins, terpenoids, phytosterols, carbohydrates, etc. [22]. Polyphenols and flavonoids are natural antioxidants and possess other pharmacological activities such as anticancer, anti-inflammatory, antianxiety, and antimicrobial [23]. The targeted extraction of plant metabolites possessing antibacterial properties can be obtained by using suitable solvents (in terms of polarity) for plant extraction [24]. The metabolites in *S. moorcroftiana* possess the potential for Ag-NPs synthesis with varying and enhanced antibacterial activity. To the best of our knowledge, no study is available that attempts to synthesize and study Ag-NPs synthesized through this plant using different solvents. Thus, this research study focuses on the antibacterial activity and bioreduction potential of *S. moorcroftiana* extracts based on highly polar (Water), less polar (Dimethyl Sulfoxide), and nonpolar (n-hexane) solvents. The purpose of our current study was to determine the effect of the polarity of solvents and the extraction method on the extraction of biologically important phytochemicals of *S. moorcroftiana* and the synthesis of Ag-NPs (Fig 1). This study further aims to comparatively analyze Ag-NPs synthesized from the extracts of *S. moorcroftiana* in different solvents, in terms of stability, morphology, functional groups, surface charge, and activity against multi-drug resistant bacteria.

2. Materials and methods

2.1 Plant material and preparation of extract

Fresh *Salvia moorcroftiana* leaves were collected from the district of Swat, Khyber Pakhtunkhwa, Pakistan. The plant was shade dried and ground into fine powder for extraction. Three types of extracts were prepared in different solvents ranging from polar to nonpolar: aqueous extract (Aq-extract), DMSO-based extract (D-extract), and hexane-based extract (H-extract).

2.1.1 Preparation of aqueous extract. Aqueous extract of *S. moorcroftiana* was prepared by mixing 5 g of plant powder with 100 mL distilled water. The mixture was boiled for 10min and cooled at room temperature. The solution was filtered through Whatman (2.5 μm) filter paper to completely remove the plant remains. The resultant extract was stored at 4˚C for further use.

2.1.2 Dimethyl sulfoxide-based extraction. The DMSO-based extract was prepared by mixing 2 g of plant powder with 50 mL DMSO. The mixture was sonicated for 30 min. Whatman (2.5 μ) filter paper was used to filter the mixture to remove plant debris. The dark green viscous plant extract in DMSO was obtained.

2.1.3 Hexane-based extraction. The hexane-based extract was prepared by mixing 5 g of plant powder with 100 mL of hexane. The mixture was heated in the water bath at 60˚C for 20

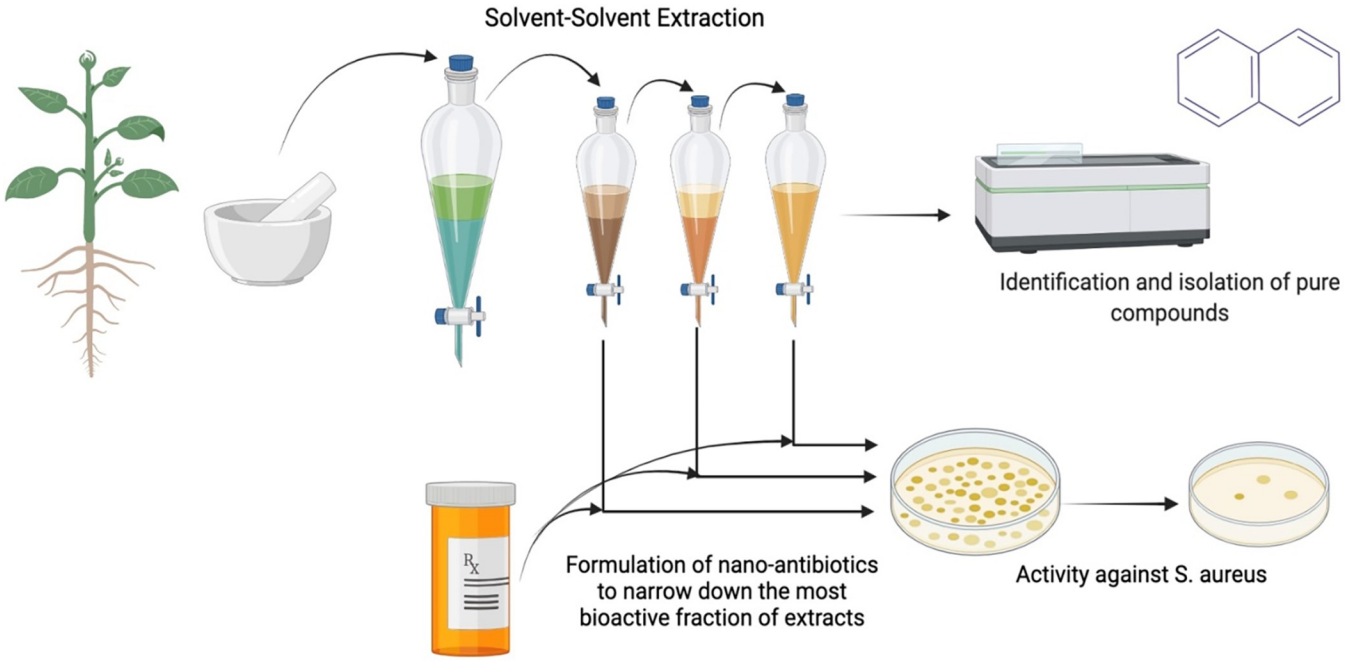


Fig 1. Solvent-based extraction of antimicrobial phytochemicals.

https://doi.org/10.1371/journal.pone.0287080.g001

min and then agitated in a shaker for 30 min. The mixture was filtered through Whatman filter paper. The thin hexane-based extract with light green color was obtained.

2.1.4 Solvent-solvent fractional extraction of *Salvia moorcroftiana*. To separate phytochemicals based on their relative solubility liquid-liquid extraction was used. 5 g of plant powder was mixed in 100 mL hexane which was then heated at 60˚C for 20 min, agitated for 30 min in a shaker, and then filtered through the Whatman filter to extract the nonpolar components of the plant. The filtrate was stored at 4˚C and the plant debris was used for further extraction. To the remaining plant debris, 100 mL DMSO was added and sonicated for 30 min. The mixture was filtered through the Whatman filter. The filtrate termed DMSO*-extract was stored at 4˚C. To the remaining plant debris, 100 mL distilled water was added and boiled for 10 min. Subsequently, the mixture was filtered and Aq*-extract was obtained that was stored for further use.

2.2 Biosynthesis of silver nanoparticles

Ag-NPs were synthesized in all fractions of extracts of *S. moorcroftiana*. For the synthesis, both aqueous extracts i.e. obtained directly from intact plant material (Aq-extract) and through solvent-solvent extraction (Aq*-extracts) were mixed with 4 mM solution of Silver nitrate ($AgNO_3$) in clean flasks in a specific ratio (1:2). This means to 100 mL aqueous plant extract 200 mL $AgNO_3$ solution was added. The solution was incubated in daylight for 3 h. Similarly, DMSO-based extracts obtained directly from intact plant powder (D-extract) and through solvent-solvent extraction (D*-extracts) were mixed with $AgNO_3$ solution in 1:6. This means that 20 mL DMSO-based extract was mixed with 120 mL $AgNO_3$ solution. The solution was incubated in daylight for 4 h. The hexane-based extract (30 mL) was dried in the oven at 50˚C for about 6 h. After this, an oily semi-dried extract was obtained. Methanol, due to its known ability to extract a broad range of phytochemicals was used to dissolve compounds from dried hexane extract. 20 mL methanol was added to the dried hexane extract and the mixture was

vortexed for 15 min followed by sonication for 5 min. The resultant methanolic extract was filtered (Whatman filter) to remove clumps. Finally, 30 mL of 4mM $AgNO_3$ solution (synthesized in methanol) was added to 15 mL methanolic extract and incubated for 24 h.

The synthesis of Ag-NPs was observed in each of the extracts by a change in color. Synthesis in aqueous extract changed the color of the solution from light brown to reddish brown; in DMSO extract the color changed from light green to dark brown, and in hexane extract the color changed from lime to light grey. The Ag-NPs synthesized in all the extracts were obtained through centrifugation at 13000 rpm for 10 min. The pellet (nanoparticles) was dried in the oven at 50˚C for 24 h, collected, and stored.

2.3 Characterization and confirmation of silver nanoparticles

Characterization of all types of Ag-NPs was carried out. These nanoparticles included Ag-NPs synthesized in aqueous extract of *S. moorcroftiana* (Aq-Ag-NPs), in aqueous fraction (Aq*-Ag-NPs), in DMSO based extract (D-Ag-NPs), and DMSO based fraction (D*-Ag-NPs).

2.3.1 UV-Visible spectroscopy. The biosynthesis of Ag-NPs was confirmed by measuring absorbance using UV-Visible spectroscopy (BKS360 BIOBASE Spectrophotometer). 1 mL of each sample of the reaction mixture (after the reaction of $AgNO_3$ and plant extract) was scanned in a spectrophotometer with the wavelength ranging from 300–600 nm. Each of the respective plant extracts was taken as a control. The solvents used for the synthesis of Ag-NPs were taken as a reference for Ag-NPs synthesized in aqueous extract water was used as a reference.

2.3.2 Fourier transform infrared spectroscopy. FTIR characterizes the biomolecules involved in the formation and stabilization of Ag-NPs. To indicate the phytochemicals involved in the capping of Ag-NPs in each of the extracts of *S. moorcroftiana* including aqueous extracts i.e., Aq-extract, Aq*-extract D-extract, and D*-extract. All types of Ag-NPs (2 mg) in their dried form were ground with potassium bromide (KBr) pellets. For appropriate results verification, scanning was done at a 1:100 ratio followed by recording a spectrum at a wavelength of 4500 to 500 cm^{-1}. The different modes of vibrations of functional groups were identified and associated with the belonging biomolecules.

2.3.3 Transmission electron microscopy and particle size analysis through Image J. The size and shape of biosynthesized Ag-NPs were calculated and visualized through TEM. 2 μL of Ag-NPs suspension were dropped onto 400 mesh carbon-coated copper grid. The suspension was dried under a lamp in ambient conditions to form a thin layer. Afterward, the samples were subjected to the TEM wherein the interaction of transmitted electrons and the Ag-NPs formed images that were recorded. The average size of nanoparticles was determined by measuring the diameter of more than 50 particles on a 100 nm TEM image by using ImageJ software.

2.3.4 Dynamic light scattering of Silver nanoparticles. Dynamic Light Scattering (DLS) is a method used for the determination of the size distribution of the nanoparticles by measuring radiation scattering intensity based on the Brownian motion of particles. DLS is a non-destructive technique used to measure the size distribution and stability of silver nanoparticles in aqueous or physiological solutions. DLS uses light scattering to determine the average hydrodynamic diameter of the sample. A beam of light is put on the dispersion of nanoparticles, which scatter light to the detector. The polydispersity index (PDI) is depicted as the size distribution range of nanoparticles and their stability and uniformity. From this measurement, the mean size of particles inside the sample is obtained along with the correlation between the numbers of particles of a particular size versus the size of the nanoparticles.

2.3.5 Zeta potential determination for stability assessment. Zeta potential analysis of Ag-NPs synthesized in each aqueous and DMSO-based extract was performed to determine

their suspension stability. 3 mg Ag-NPs/5 mL dH_2O was prepared and sonicated for 30 min (Power-Sonic 405). The surface charge and hydrodynamic diameter of nanoparticle samples were analyzed using a zeta sizer (Nano-ZS ZEN 3600, Malvern) with a temperature equilibration time of 1 minute at 25˚C.

2.4 Antibacterial activity

2.4.1 Microbial strains. The antibacterial activity of each type of extract (Aq-extract, Aq*-extract, D-extract, D*-extract, and H-extract) and Ag-NPs (Aq-Ag-NPs, Aq*-Ag-NPs, D-Ag-NPs, D*-Ag-NPs, and H-Ag-NPs) was performed. The tested microorganisms include Gram-negative *Klebsiella pneumoniae* and *Pseudomonas aeruginosa*, and Gram-positive *Enterococcus faecalis* and *Staphylococcus aureus*. These are multi-drug resistant and biofilm-forming bacterial strains, thus, they are of high concern [25].

2.4.2 Disk diffusion method. The Kirby-Bauer disk diffusion assay was performed to check the antibacterial activity of nanoparticles and *S. moorcroftiana* extracts. Each of the bacterial strains was streaked on nutrient agar solidified in sterile Petri dishes. After 24 h of incubation at 37˚C, 3–5 colonies were picked using a sterile metal loop and were inoculated in fresh broth medium contained in a sterile glass tube with screw caps. The broth inoculated with bacteria was vortexed followed by 20 min incubation. The broth suspension was compared with 0.5 MacFarland standard and the turbidity was adjusted accordingly. After adjusting the turbidity of broth suspension according to the MacFarland standard indicates 1×10^8 CFU/mL of bacteria in broth. The bacteria were uniformly spread on nutrient agar in sterile petri-dishes using a sterile cotton swab dipped in broth suspension culture. The empty disks prepared from Whatman filter paper were placed on the plate (containing agar swabbed with bacteria) using autoclaved forceps. 8 μL of 2 mg/mL of each Ag-NPs and extract sample was added to each respective disc through sterile micropipette tips. The Petri dishes were sealed with parafilm and incubated for 24 h at 30˚C. The inhibition zones were recorded after 24 h of incubation.

2.4.3 Micro-dilution assay for determination of the minimum inhibitory concentration. Micro-dilution assay for each type of nanoparticles was performed to determine the minimum inhibitory concentration. The pure culture of each bacterial strain was obtained by streaking the bacteria which was incubated for 24 h at 37˚C. The colony suspension method was followed to prepare bacterial broth culture. 3–5 colonies of bacteria were picked with the help of a sterile metal loop and were inoculated in a fresh broth medium. The bacterial broth culture was compared with 0.5 MacFarland standard by comparing the optical density (OD) at 625 nm. The absorbance was observed in the range of 0.08–0.13 which is the desired value and indicates approximately 1×10^8 CFU/ mL. 8 mg/mL stock solution of Aq-Ag-NPs, Aq*-Ag-NPs, D-Ag-NPs, D*-Ag-NPs, and 4 mg/mL H-Ag-NPs (stock solution) was prepared. The stock solutions were twofold diluted up to the 10^{th} well. The concentrations of Aq-Ag-NPs, Aq*-Ag-NPs, D-Ag-NPs, and D*-Ag-NPs started at 4 mg/ml and ended at 7.8 μg/mL. However, H-Ag-NPs the concentrations started from 2 mg/ml and ended at 3.9 μg/mL.

The dilutions were added to their respective wells of a 96-well microtitre plate. A separate plate was used for each of the bacteria. 50 μL of bacterial broth culture was added from the 1^{st} to 11^{th} (growth control) column. 50 μL of broth (only) was added to the 11^{th} column and 100 μL to the 12^{th} (sterility control). The plate was incubated for 20 h at 37˚C in a shaking incubator. The MIC was observed visually by determining the concentration at which Ag-NPs inhibited the bacterial growth resulting in a clear well.

2.4.4 Mechanism of bacterial inhibition by the biosynthesized Ag-NPs. The oxidant sensitive probe 2', 7'-dichlorodihydroluorescein diacetate (H_2DCFDA) was used to determine

the intracellular levels of ROS in cells treated with different concentrations of Ag-NPs (0.5–250 μg/mL). Bacterial cells were grown in an LB medium until OD_{600} reaches 0.5. The bacterial cultures were centrifuged to pellet the cells. The cells were washed with 10 mM potassium phosphate buffer (pH 7.0) through vortexing and centrifugation. After washing, the cells were suspended in the same buffer and disrupted by sonication. 10 mM H2DCFDA (dissolved in dimethyl sulfoxide) was added at a ratio of 1:2000 (2 microliters in 4 mL buffer), followed by shaking for 30 min at 37˚C. The bacterial cells were again pelleted after incubation through centrifugation. The cells were washed two times with the same buffer to remove the H_2DCFDA. To cell suspension, different concentrations Ag-NPs were applied. The fluorescence intensity of DCF by fluorescence spectrophotometer at an excitation wavelength of 488 nm and an emission wavelength of 535 nm was measured.

2.5 Comparative analysis of phytochemical content in extracts and Silver nanoparticles

2.5.1 Determination of total phenolic content. Phenolics are antioxidant molecules with pharmacological activities and reducing capabilities. The total phenolic content in each of the extracts and Ag-NPs synthesized from these extracts were determined quantitatively by using the Folin Ciocalteu method with gallic acid as the standard. Briefly, 20 μL of each extract and Ag-NPs sample (2 mg/mL) were added to a 96-well plate. Then, 90 μL Folin Ciocalteu reagent (1:10 diluted form) was added to the sample. Subsequently, 90 μL of 6% sodium carbonate was added. Gallic acid (4 mg/mL stock in methanol) was used as a standard positive control. The plate was incubated for 30 min and then the optical density of total phenolic content was measured at 630 nm.

2.5.2 Determination of total flavonoid content. Similar to phenolics, flavonoids possess great medicinal importance and reducing potential. They also show reduction and stabilization potential in the synthesis of Ag-NPs. The total flavonoid content was measured using the Aluminium chloride ($AlCl_3$) method. Briefly, 20 μL of each of the extract and Ag-NPs (2 mg/mL) sample were added to a 96-well plate. Potassium acetate (10 μL of 98.15 g/L) was added followed by the addition of 10 μL aluminum chloride (10 g/100 mL). Subsequently, 160 μL of distilled water was added. The 20 μL MeOH instead of the sample was used as a negative control. The plate was incubated for 30 min and then the optical density was measured at 405 nm.

2.5.3 DPPH (2,2-diphenylpicrylhydrazyl) assay. A DPPH assay was performed to assess the free radical scavenging activity (FRSA) of *S*. *moorcroftiana* extracts and Ag-NPs synthesized from it. DPPH is a stable free radical; therefore, it is used to assess whether the extracts and Ag-NPs possess the ability to scavenge this radical. To determine the antioxidant activity 20 μL of sample (extracts and 2 mg/mL Ag-NPs) was added to a 96-well plate. Then, 180 μL of DPPH reagent (3.2 mg/100 mL) was added subsequently. Ascorbic acid (4 mg/mL) was used as positive control which is a naturally free radical scavenging agent. The plate was incubated for 1 hr and FRSA was measured by recording absorbance at 517 nm.

2.5.4 Oxidation-reduction potential. The ORP of extracts was determined to know their reduction potential in the synthesis of Ag-NPs. The ORP of Ag-NPs was determined to analyze the potential of nanoparticles as oxidative species that are lethal for bacteria. The ORP was measured through an ORP sensor probe lubricated with potassium chloride. The rod was dipped in each of the extracts and the ORP for each extracted sample was measured three times subsequently their average was considered as a final value. A similar procedure was done to determine the ORP of all Ag-NPs solution (2 mg/ml). The probe was rinsed with distilled water every time it was used for different kinds of extract and Ag-NPs solution.

2.6 High-Performance Liquid Chromatography (HPLC) for identification of polyphenols in plant extracts

HPLC quantification was carried out according to a reported method (Zeb 2015). Briefly, 1-g powdered sample of each of the whole and fractionated extract was added to water and methanol in equal ratios, and the mixture was subject to heating in a water bath at 70˚C for 1 h. The mixture was then filtered through a non-pyogenic 0.4 μm CA syringe filter.

To identify and quantify phenolic compounds the Agilent-1260 infinity High-performance liquid chromatography (HPLC) system was used. The HPLC system's essential parts were a quaternary pump, an auto-sampler, a degasser, and a C18 column (Agilent-Zorbax-Eclipse column). The solution (B and C) gradient was such that solvent B was a mixture of acetic acid: methanol: deionized water (20: 100: 180 v/v), and solvent C was a mixture of acetic acid deionized water: methanol (20: 80: 900) v/v. The solvents were provided as a gradient such that they started and gradually decreased the solvent in concentration. Solvent B was given in volume 100, 85, 50, and 30% at 0, 5, 20, and 25 min, finally giving way to 100% solvent C from 30 min onwards till 40 min. The ultraviolet array detector (UVAD) was set at wavelength 250 nm to analyze phenolic compounds, and the chromatograms were recorded. Phenolic compounds were identified by comparing the retention times of obtained HPLC chromatogram with that of the standards.

3. Results and discussion

3.1 Synthesis of silver nanoparticles in plant extracts obtained in solvents with varying polarity

The biosynthesis reaction of Ag-NPs was performed in each of the extracts by allowing it to react with the $AgNO_3$ solution. After 4 h of reaction, a color change was observed that was different for each of the extracts. The color change is a characteristic determining the reduction of Ag^+ by plant metabolites [26]. This color change is due to the interaction of light and the surface oscillating electrons of silver nanoparticles, the phenomenon is known as surface plasmon resonance [27]. Thus, each of the extracts either whole or fraction had the potential of Ag-NPs synthesis except for H-extract. A very slow reaction and thus synthesis of Ag-NPs were observed in hexane because it is nonpolar and is usually used for the extraction of nonpolar compounds. $AgNO_3$, being polar cannot react with nonpolar compounds. The dried H-extract was dissolved in methanol because of its good extraction capability [28]. As a result, H-extract dissolved in methanol when reacted with $AgNO_3$ solution, and a very low concentration of synthesized Ag-NPs was observed.

3.2 UV-Vis spectroscopy of silver nanoparticles

UV-Vis absorption spectra of the biosynthesized Ag-NPs showed the characteristic surface plasmon resonance of Ag-NPs in the range of 400–500 nm, confirming their synthesis [29]. Surface plasmon resonance refers to the phenomenon where electron clouds around Ag-NPs can oscillate and absorb specific wavelengths of electromagnetic radiation. Such absorbance is the result of the size of nanoparticles along with other factors including condition of synthesis, solvent, and surface functionalization [30]. Based on the sizes and solvent used, various absorption bands were observed for each kind of nanoparticles (shown in Fig 2).

The maximum absorbance (represented as $\lambda_{(max)}$) in the range of 400–500 was recorded to be 498 nm for Aq-Ag-NPs, 432 nm for D-Ag-NPs, and 414 nm for H-Ag-NPs (Fig 2A). [29]. Aq-Ag-NPs and D-Ag-NPs showed broader peaks indicating the presence of nanoparticles with varying sizes [31]. H-Ag-NPs gave a narrow SPR band with little absorption intensity that

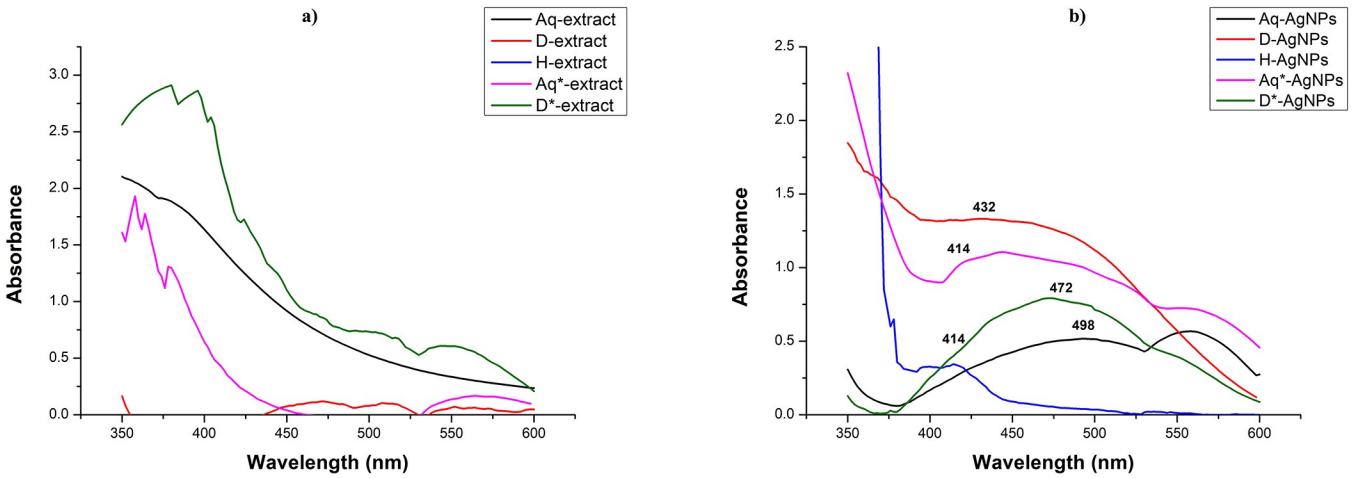


Fig 2. UV-Vis spectra of (a) *S. moorcroftiana extracts* and (b) silver nanoparticles synthesized from these extracts.

https://doi.org/10.1371/journal.pone.0287080.g002

shows a small concentration of biosynthesized H-Ag-NPs [31]. With the increase in the size of nanoparticles, the absorbance intensity decreases [32] as observed with Aq-Ag-NPs when compared with D-Ag-NPs. Kochkina and Skobeleva [33] synthesized Ag-NPs from the reaction of starches dissolved in DMSO with $AgNO_3$ and observed the surface plasmon band maximum at 418 nm. The absorption bands of Aq*-Ag-NPs ($\lambda_{(max)}$ = 414 nm) and D*-Ag-NPs ($\lambda_{(max)}$ = 472 nm) within the characteristic range confirms their presence. The UV-Vis spectra of *S. moorcroftiana* extract in different solvents are taken as control (Fig 2B) to compare their absorption peaks with that of Ag-NPs. Although the extracts showed absorbance in the UV-Vis range, no characteristic peaks are found to be similar to the peaks of Ag-NPs. The D-shaped absorption curve of D*-Ag-NPs in the range of 400–500 is indicative of the presence of Ag-NPs in the sample when compared to D*-extract whose absorption showed to be continuously decreasing within this range. According to the absorption spectra of various types of Ag-NPs, most of the Ag-NPs were spherical because their absorption peaks were mostly in the range of 400–470 nm which refers to spherical-shaped nanoparticles, with sizes less than 20 nm [34]. These results agree with the results of TEM. Thus UV-Vis spectroscopy results clearly show that the synthesis of Ag-NPs from their respective extracts is achieved.

3.3 Fourier Transform Infra-Red Spectroscopy (FTIR)

Generally, the FTIR spectra of the given plant extracts and Ag-NPs revealed that the compounds present in the extracts have capped the biosynthesized Ag-NPs (as shown in Fig 3) and therefore, gave peaks in the same range of wavenumbers. However, less absorption and more transmittance were observed in the FTIR spectra of Ag-NPs than that of extracts from which they were synthesized.

The FTIR spectra of Aq-extract and Aq-Ag-NPs (Fig 4A) revealed the absorption of infrared waves by the same functional groups within the same wavenumber range. A broad bend was observed between 3400–3154 cm^{-1} (96% transmittance) for Aq-extract and 3380–3190 cm^{-1} (98% transmittance) for Aq-Ag-NPs that attributed to the presence of OH stretching (corresponding to alcohol). Also, the peaks could be seen at 2980 cm^{-1} (95% transmittance), 2951 cm^{-1} (95% transmittance) and 2972 cm^{-1} (98% transmittance), and 2920 cm^{-1} (97% transmittance) for Aq-extract and Aq-Ag-NPs, respectively. All these peaks fall in the range which represents the presence of N-H (amine) and C-H (alkane) functional groups, correspondingly.

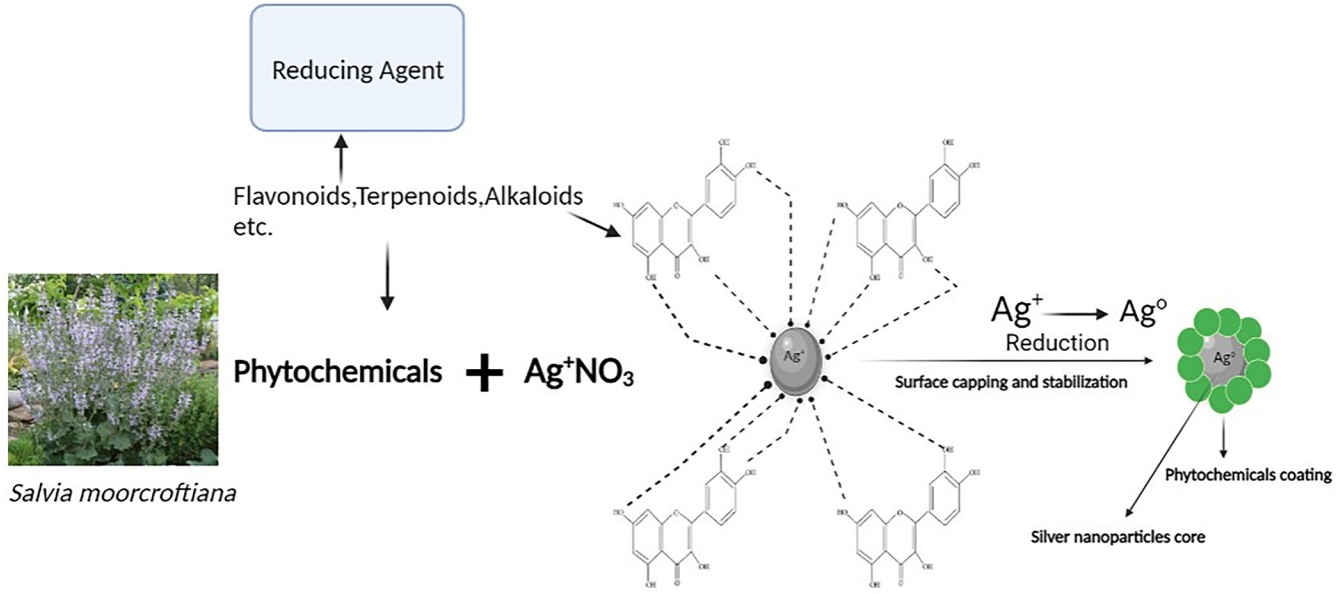


Fig 3. Schematic illustration for Ag-NPs reduction and capping through phytochemicals.

https://doi.org/10.1371/journal.pone.0287080.g003

Further, absorption peaks were observed at 1589 cm^{-1}, 1060 cm^{-1}, and 1034 cm^{-1} (91%, 88%, 88% transmittance, respectively) for Aq-extract and 1629 cm^{-1}, 1060 cm^{-1}, and 1055 cm^{-1} (97%, 96%, 96% transmittance, respectively) for Aq-Ag-NPs. These peaks revealed the occurrence of N-H bending (amine), S = O, and C-O stretching (representing sulfoxide and alcohol groups). A broad peak within the range of 3578–3000 cm^{-1} was observed in the spectrum of D-extract (Fig 4C) along with other noticeable peaks at 1634 cm^{-1}, 1047 cm^{-1}, and 1019 cm^{-1}. Similarly, for D-Ag-NPs a broad peak was shown within the range of 3500–3100 cm^{-1}, and sharp peaks at 1654 cm^{-1}, 1615 cm^{-1}, and 1030 cm^{-1}. The above-mentioned absorption bands are attributed to the presence of OH and N-H stretching (corresponding to alcohol and amines), C-H (alkanes), C = C (conjugated alkenes), and C-N (amines). The FTIR spectrum of Aq*-extract (Fig 4B) within the range of 3524–3040 cm^{-1} showed absorbance (67% transmittance) by showing a broad peak, while in Aq*-Ag-NPs in the specified range a little absorbance was observed with a slight bend at 3300 cm^{-1} (72% transmittance). This is attributed to the presence of OH stretching corresponding to the alcohol group. Furthermore, Aq*-extract gave observable peaks at 2941 cm^{-1} (79% transmittance), 1596 cm^{-1} (44% transmittance), 1404 cm^{-1} (54% transmittance), and 1019 cm^{-1} (48% transmittance). The peaks for Aq*-Ag-NPs were

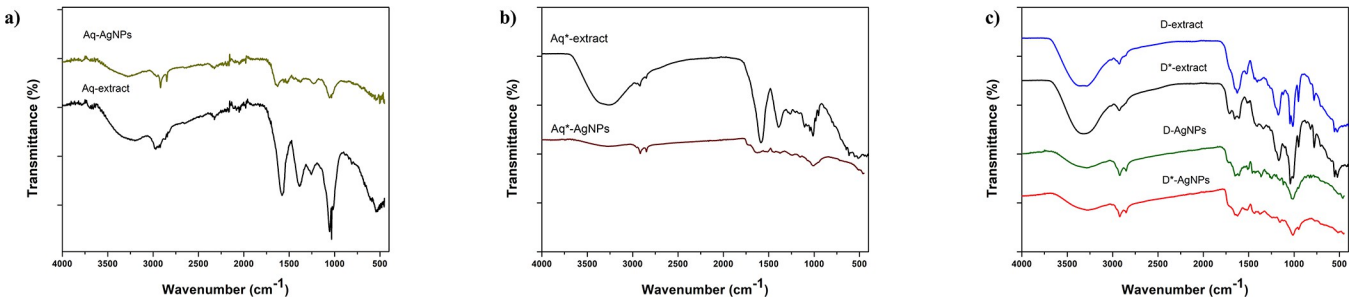


Fig 4. FTIR spectra of a) Aq-extract and Ag-NPs b) Aq*-extract and Ag-NPs c) D-extract and Ag-NPs, D*-extract and Ag-NPs.

https://doi.org/10.1371/journal.pone.0287080.g004

observed at 2920 cm^{-1} (68% transmittance), 1652 cm^{-1} (68% transmittance), 1400 cm^{-1} (68% transmittance), and 1000 cm^{-1} (60% transmittance). These peaks represent the presence of OH stretching (alcohol), C-H stretching (alkane), C = C stretching (alkene), S = O stretching (sulfate), and C-F (fluoro compound) respectively, for both extract and Ag-NPs. A broad peak in spectra of D*-extract and D*-Ag-NPs (Fig 4C) within the range of 3412–3216 cm^{-1} (66% transmittance) and 3434–3226 cm^{-1} (68% transmittance) representing the presence of OH stretching corresponding to an alcohol group. Other noticeable peaks could be seen for D*-extract and Ag-NPs at 1663 cm^{-1} (76% transmittance) and 1660 cm^{-1} (66% transmittance), 1178 cm^{-1} (50% transmittance), and 1168 cm^{-1} (62% transmittance), 1045 cm^{-1} (36% transmittance) and 1027 cm^{-1} (54% transmittance). The absorption at these wavenumbers showed the presence of OH stretching (alcohol), C = C (alkene), C-O stretching (ester), and C-N stretching (amine), respectively.

The presence of these functional groups indicates the presence of polyphenols (such as flavonoids and phenolics), terpenoids, carboxylic acid, amines in proteins, aromatic amines, alkenes, alkanes, and organosulfur compounds attached to the surface of Ag-NPs. The presence of these phytochemicals in both the plant extracts and Ag-NPs indicates their role in the synthesis and stabilization of Ag-NPs [35–37]. It is challenging to point out a single specific class of phytochemicals involved in the synthesis of Ag-NPs, but generally, all these compounds are significant for the synthesis of silver nanoparticles [38]. These phytochemicals possess antibacterial properties and can result in the synthesis of Ag-NPs with enhanced antibacterial activity [39]. Only D*-extract and D*-Ag-NPs showed a distinctive peak at 1168 cm^{-1} and 1178 cm^{-1} indicating C-O vibration corresponding to esters. In previous studies, it has been shown that ester molecules were obtained in high concentration through extraction in polar solvents as compared to nonpolar [40]. Moreover, both aqueous whole and fraction extracts and Ag-NPs based on them revealed the presence of sulfate or sulfoxide (S = O) which is the functional group of organosulfur compounds in plants [41]. This compound was not found in DMSO-based extracts and Ag-NPs because they are known to decompose in DMSO [42].

3.4 Transmission electron microscopy of silver nanoparticles

TEM was used to analyze the morphology of biosynthesized Ag-NPs. The TEM images confirmed the synthesis of Ag-NPs in all the extracts of *S. moorcroftiana* (Fig 5). The nanoparticles in all the extracts appeared to be polydispersed having both large and small diameters with average diameters of 17.889, 17.11, 18.82, and 17.815 nm for Aq-Ag-NPs, D-Ag-NPs, Aq*-Ag-NPs, and D*-Ag-NPs, respectively (Table 1). All of the biosynthesized Ag-NPs were almost spherical as determined by TEM micrographs. Ag-NPs with smaller sizes and spherical morphology are more effective against bacteria because they can easily attach and enter the cells via membranes leading to bactericidal effects [4]. The close analysis of images showed that clusters of nanoparticles are surrounded by a layer. Such layers are found around nanoparticles mainly synthesized from medicinal plant extracts, where the phytochemicals form a capping layer and help to shape the particles during growth [43].

3.5 Zeta potential data for assessing the stability of silver nanoparticles

Zeta potential, the electrostatic repulsion or attraction between the particles is determined through Dynamic Light Scattering (DLS). The negative or positive zeta values indicate the repulsive force between the particles showing dispersity and stability. All types of samples showed negative zeta potential values such as -17.6±0.14 mV, -18.5±0.24 mV, -16.3±0.26 mV, and -21.8±0.16 mV for Aq-Ag-NPs, D-Ag-NPs, Aq*-Ag-NPs, and D*-Ag-NPs, respectively

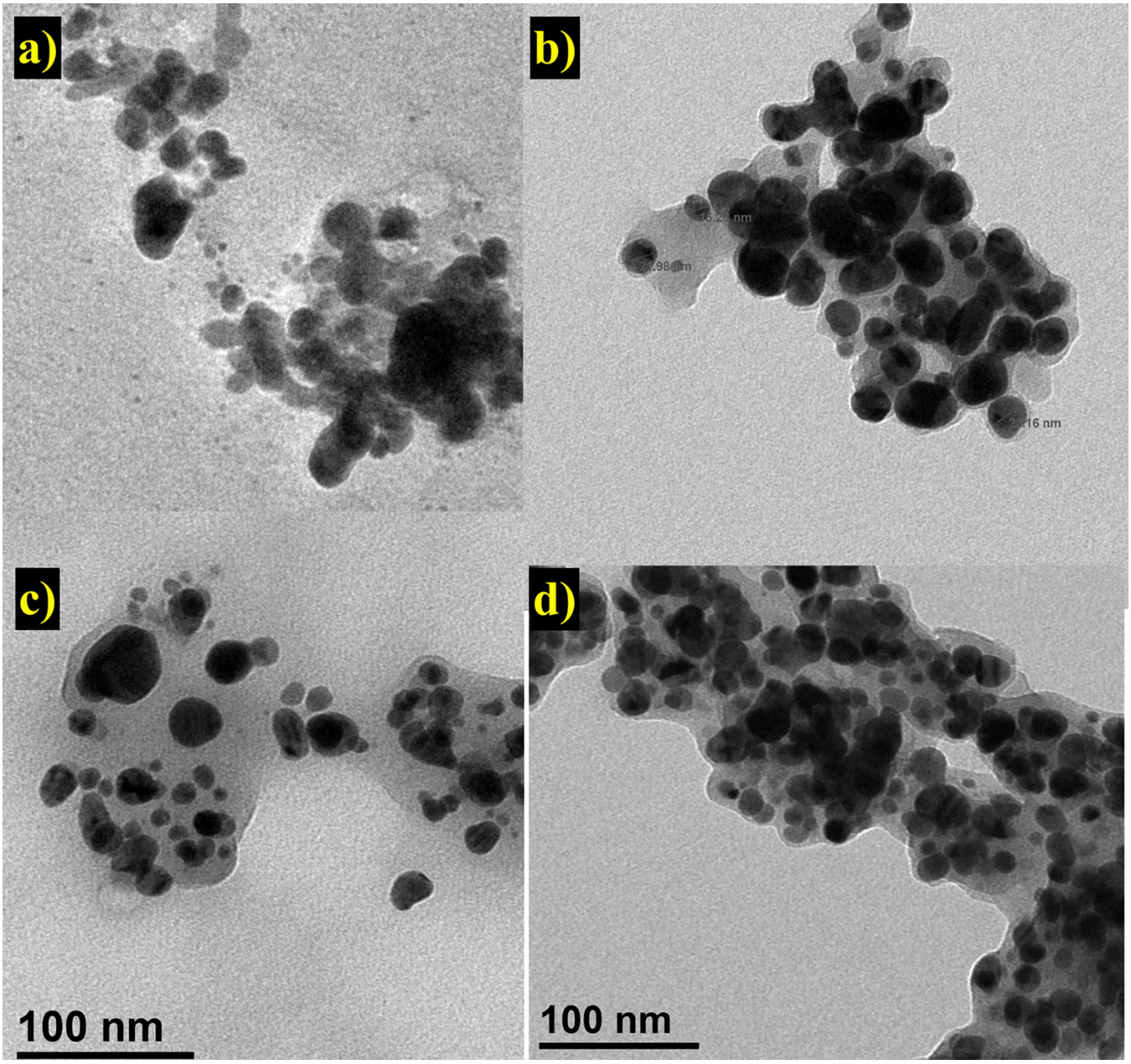


Fig 5. Transmission electron microscopy image of a) Aq-Ag-NPs, b) Aq*-Ag-NPs, c) D-Ag-NPs and d) D*-Ag-NPs.

https://doi.org/10.1371/journal.pone.0287080.g005

Table 1. Combined Table of size and stability-based characteristics of silver nanoparticles.

Types of Ag-NPs	PDI	Hydrodynamic Size (nm)	Zeta potential (mV)	TEM (nm)
D*-Ag-NPs	0.335	377	-21.8±0.16	17.815
D-Ag-NPs	0.266	365	-18.5±0.24	17.11
Aq*-Ag-NPs	0.5	99.36	-16.3±0.26	18.82
Aq-Ag-NPs	0.373	135.7	-17.6±0.14	17.889

https://doi.org/10.1371/journal.pone.0287080.t001

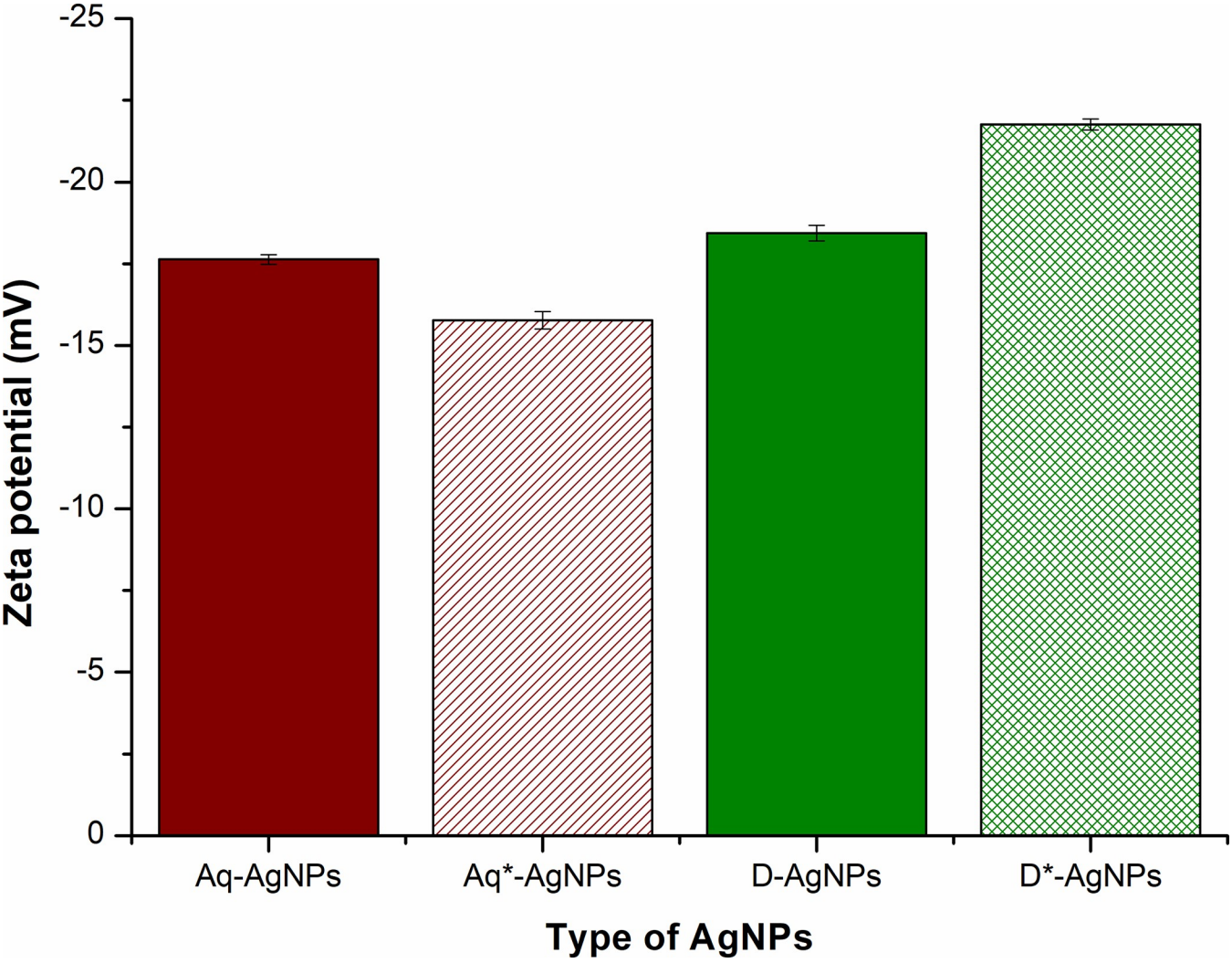


Fig 6. Determination of Zeta potential of silver nanoparticles synthesized via different solvents.

https://doi.org/10.1371/journal.pone.0287080.g006

(Fig 6). The negative zeta potential values indicated that the Ag-NPs possessed a positive charge in the solution that attracted negative charges to surround them [44]. The negative zeta values also indicate the repulsive force among the nanoparticles, hence confirming their stability [45]. In this context, the DMSO plant extract-based Ag-NPs were found to be more stable than the aqueous one. Furthermore, between the DMSO plant extract-based Ag-NPs, D*-Ag-NPs were revealed to be more stable with zeta value = -21.8±0.16 mV.

3.6 Size distribution of silver nanoparticles determined through Dynamic light scattering

DLS was used to determine the polydispersity index, referring to the size distribution of nanoparticles in solution. Furthermore, hydrodynamic size or average zeta size was also calculated for four types of Ag-NPs i.e. Aq-Ag-NPs, D-Ag-NPs, Aq*-Ag-NPs, and D*-Ag-NPs (Fig 7). The values of the mentioned characteristics are shown in Table 1. The results revealed the average zeta size of Aq-Ag-NPs, D-Ag-NPs, Aq*-Ag-NPs, and D*-Ag-NPs to be 135.7 d. nm, 365 d. nm, 99.36 d. nm, and 377 d. nm, respectively. All the Ag-NPs were found to be less

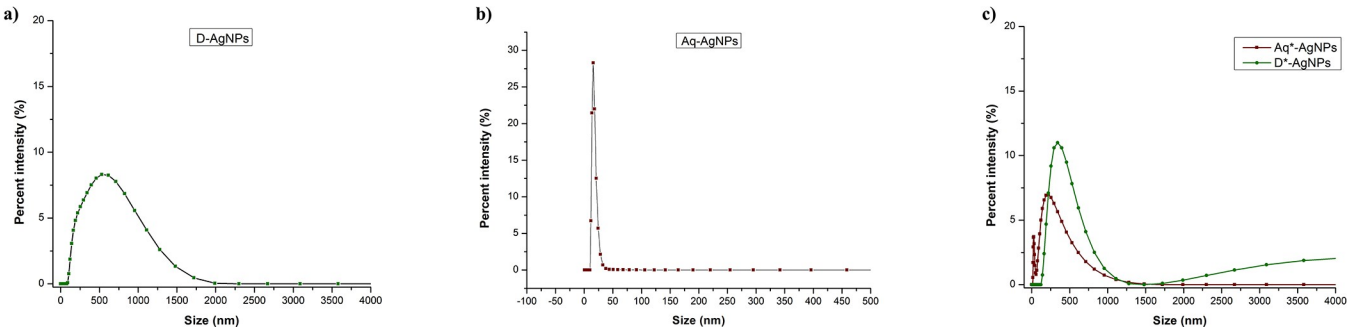


Fig 7. Size distributions of silver nanoparticles synthesized via different extracts.

https://doi.org/10.1371/journal.pone.0287080.g007

polydispersed with the highest PDI being 0.5 recorded for Aq*-Ag-NPs followed by Aq-Ag-NPs with 0.373 PDI, D*-Ag-NPs with 0.335 PDI, and D-Ag-NPs with the lowest PDI (0.26). The size determined by DLS was found to be larger than the size determined by TEM because it measures the hydrodynamic size of nanoparticles rather than their physical diameters [46]. This means that during the movement of nanoparticles in a liquid medium, the electric dipole layer of the solvent surrounds them which can also influence their motion in the solvent. Thus, hydrodynamic diameter shows the combined diameter of the metal core and the solvent molecules surrounding it [47]. In this context, DMSO-based Ag-NPs are probably surrounded by more protective layers than aqueous extract-based Ag-NPs, thus having large hydrodynamic diameter.

3.7 Comparative analysis of phytochemical content in plant extracts and Silver nanoparticles

3.7.1 Total phenolic content in extracts and silver nanoparticles. The TPC and TFC results showed that high amount of phenolic and flavonoid compounds are present in the extracts which act as reducing and capping agents utilized in the synthesis of stable Ag-NPs [48]. The TPC and TFC of Ag-NPs gave evidence of the capping and stabilizing capability of these compounds [49] showing that during synthesis, they attach to the Ag-NPs to stabilize them and provide them enhanced pharmacological properties.

TPC of extracts showed diverse results such as 98.92±4.12, 255.50±3.13, 262.48±0.84, 227.76±0.46, and 67.42±1.21 μg GAE/mL for Aq-extract, Aq*-extract, D-extract, D*-extract, and H-extract, respectively (Fig 8). The highest phenolic content was found in D-extract, followed by Aq*-extract. The least phenolics were extracted by hexane. The TPC of Ag-NPs was substantially lower than that of extracts (Fig 8). 13.01±1.19, 13.01±1.19, 26.8±1.95, and 23.44 ±0.19 μg GAE/mL are the concentrations of phenolics bound to Aq-Ag-NPs, Aq*-Ag-NPs, D-Ag-NPs, and D*-Ag-NPs, respectively. Compared to Aqueous plant extract-based Ag-NPs, D-Ag-NPs and D*-Ag-NPs had increased levels of phenolic compounds.

3.7.2 Total flavonoid content of extracts and silver nanoparticles. The flavonoids were present in higher quantity in extracts than Ag-NPs. The D-extract and D*-extract had the same and highest flavonoid content i.e., 11.42±0.54 μg QE/mL, and 11.42±0.3 μg QE/mL, respectively. TFC of Aq-extract, Aq*-extract, and H-extract was calculated to be 7.06±2.29 μg QE/mL, 5.40±0.61 μg QE/mL, and 4.72±0.13 μg QE/mL, respectively. 3.58±0.29 μg QE/mL, 9.2±0.25 μg QE/mL, 6.17±0.11 μg QE/mL, and 5.02±0.19 μg QE/mL TFC was recorded for Aq-Ag-NPs, Aq*-Ag-NPs, D-Ag-NPs, and D*-Ag-NPs. Like TPC, D and D*-Ag-NPs gave high TFC value (Fig 9).

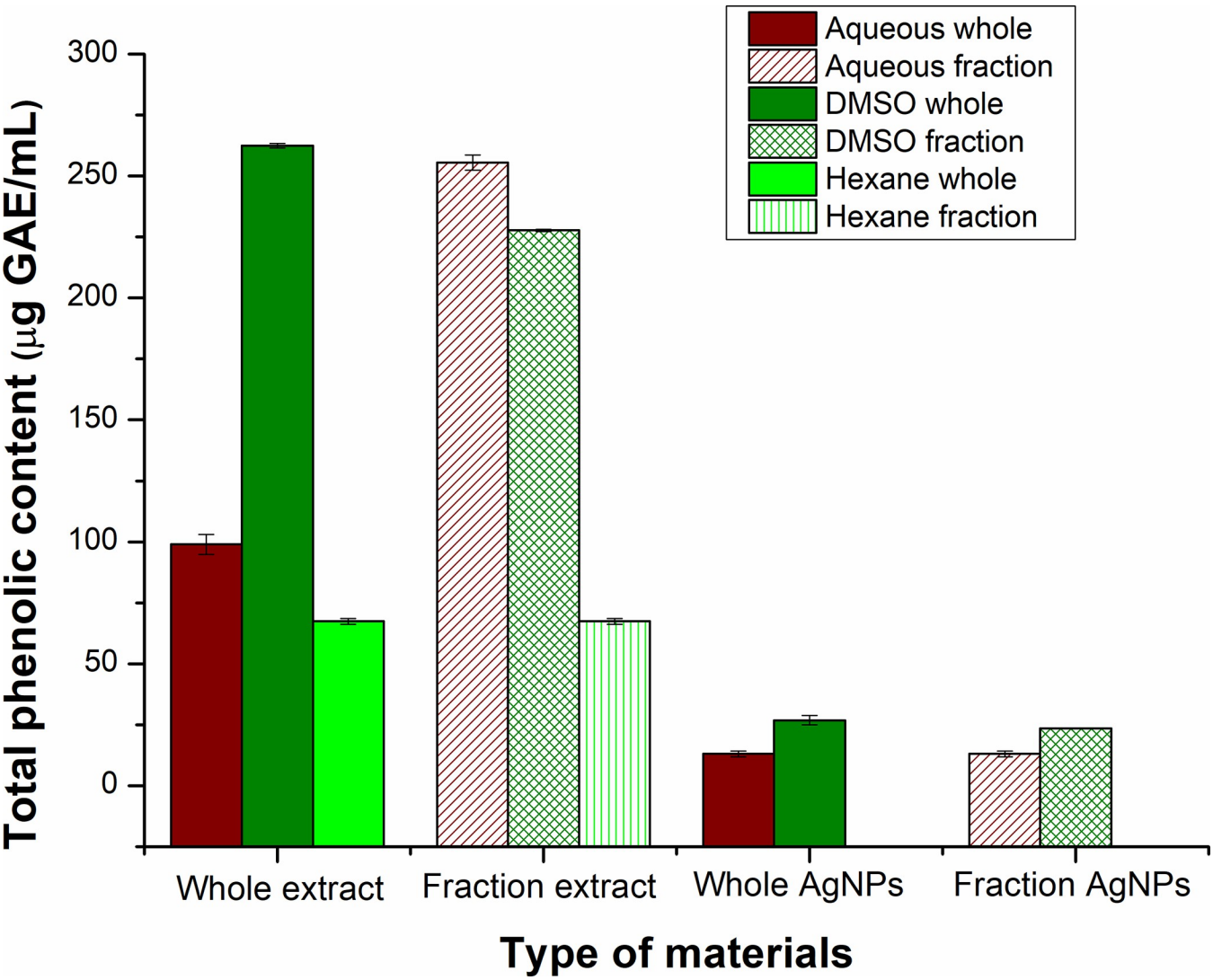


Fig 8. Comparative analysis of total phenolic content in different extracts and Ag-NPs based on different solvent-based extracts. Hexane based Ag-NPs synthesis was negligible and could not be analyzed for TPC.

https://doi.org/10.1371/journal.pone.0287080.g008

3.7.3 Antioxidant activity of extracts and silver nanoparticles. The antioxidant activity of extracts and Ag-NPs was determined by calculating their free radical scavenging activity (FRSA) (Fig 10). This free radical scavenging property is the result of reductants having reducing power that can react with and prevent the formation of free radicals [50]. The results of free radical scavenging activity indicate effective antioxidant activities of all types of extracts. This could be linked with the presence of TPC and TFC, because, phenolic compounds possess strong antioxidant potential that are found in considerable amounts in plant extracts [51]. Among the extracts, D*-extract showed the highest percent of free radical scavenging activity i.e., 80.8±0.72%, which can be attributed to the increased quantity of phenols and flavonoids extracted by DMSO in fraction. DMSO is a preferred solvent for the extraction of phenolic and flavonoid compounds as in both cases DMSO based plant extracts revealed their higher concentration. Demir, Turan [52] used DMSO for extraction of *Rhododendron luteum* and revealed its high antioxidant activity due to the extraction of higher quantities of polyphenols.

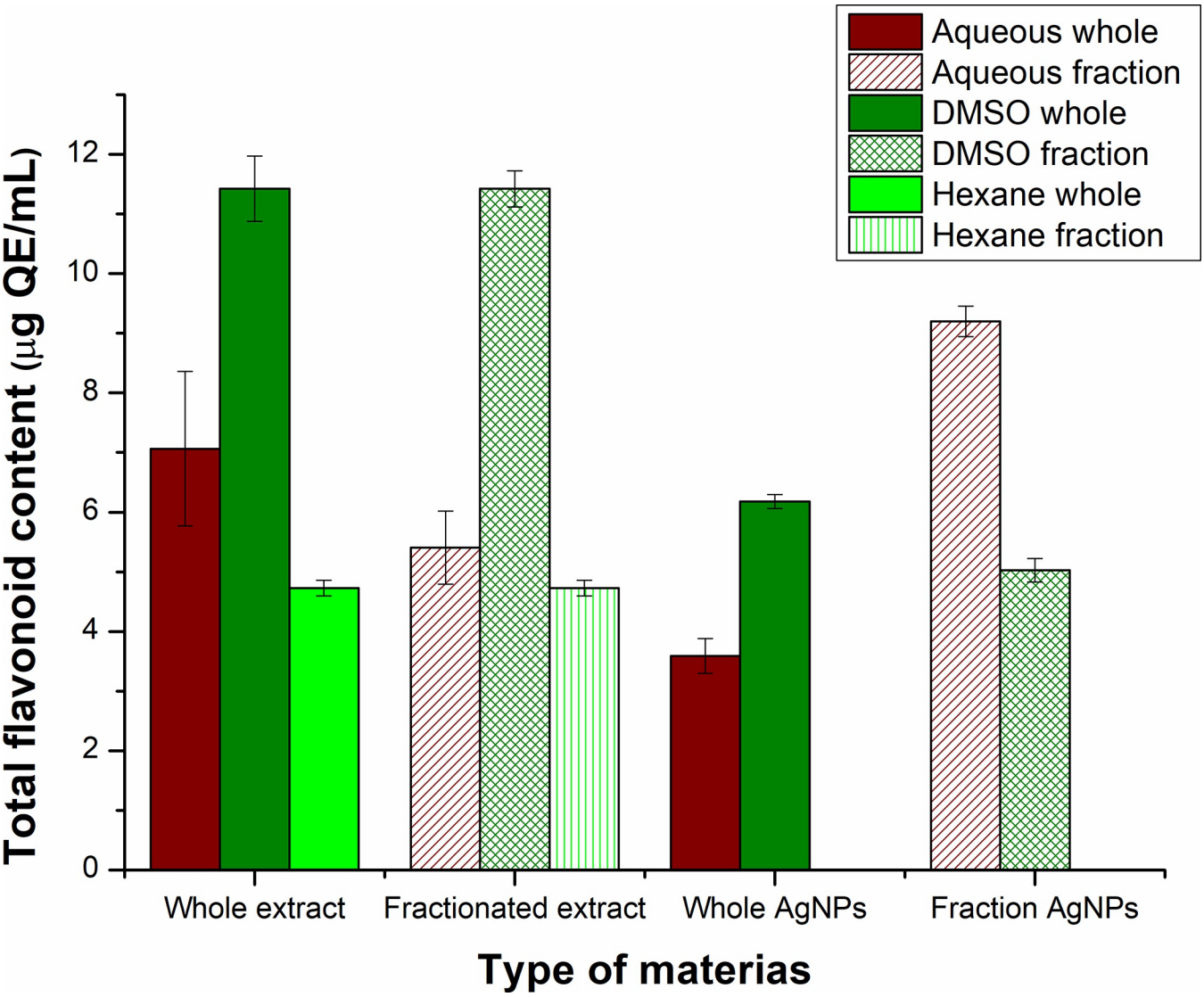


Fig 9. Comparative analysis of total flavonoid content in extracts and silver nanoparticles based on different solvent-based extracts.

https://doi.org/10.1371/journal.pone.0287080.g009

This free radical scavenging property is the result of reductants having reducing power that can react with and prevent the formation of free radicals [50]. The H-extract also revealed good antioxidant activity having 74.36±1.0 percent free radical scavenging activity.

Ag-NPs synthesized from these extracts were also found to be good antioxidant agents with the highest antioxidant potential (61±0.50%) of Aq*-Ag-NPs followed by D*-Ag-NPs with 56 ±1.55% FRSA. This reveals that Ag-NPs synthesized from fractionated plant extracts was higher as compared to the one synthesized from whole extracts. Thus, the strategy of fractionated plant extraction and the synthesis of Ag-NPs from these extracts result in the production of good antioxidant agents.

3.7.4 Oxidation Reduction potential of extracts and silver nanoparticles. ORP of extracts was determined to find the reducing agents and their reduction potential for the synthesis of Ag-NPs. The more negative is the value the more reducing agents are present in the extract having the capability to reduce Ag^{+} to Ag-NPs indicating high reduction potential [53]. The highest reduction potential was recorded for Aq-extract (-113.667±1.17 mV) and the

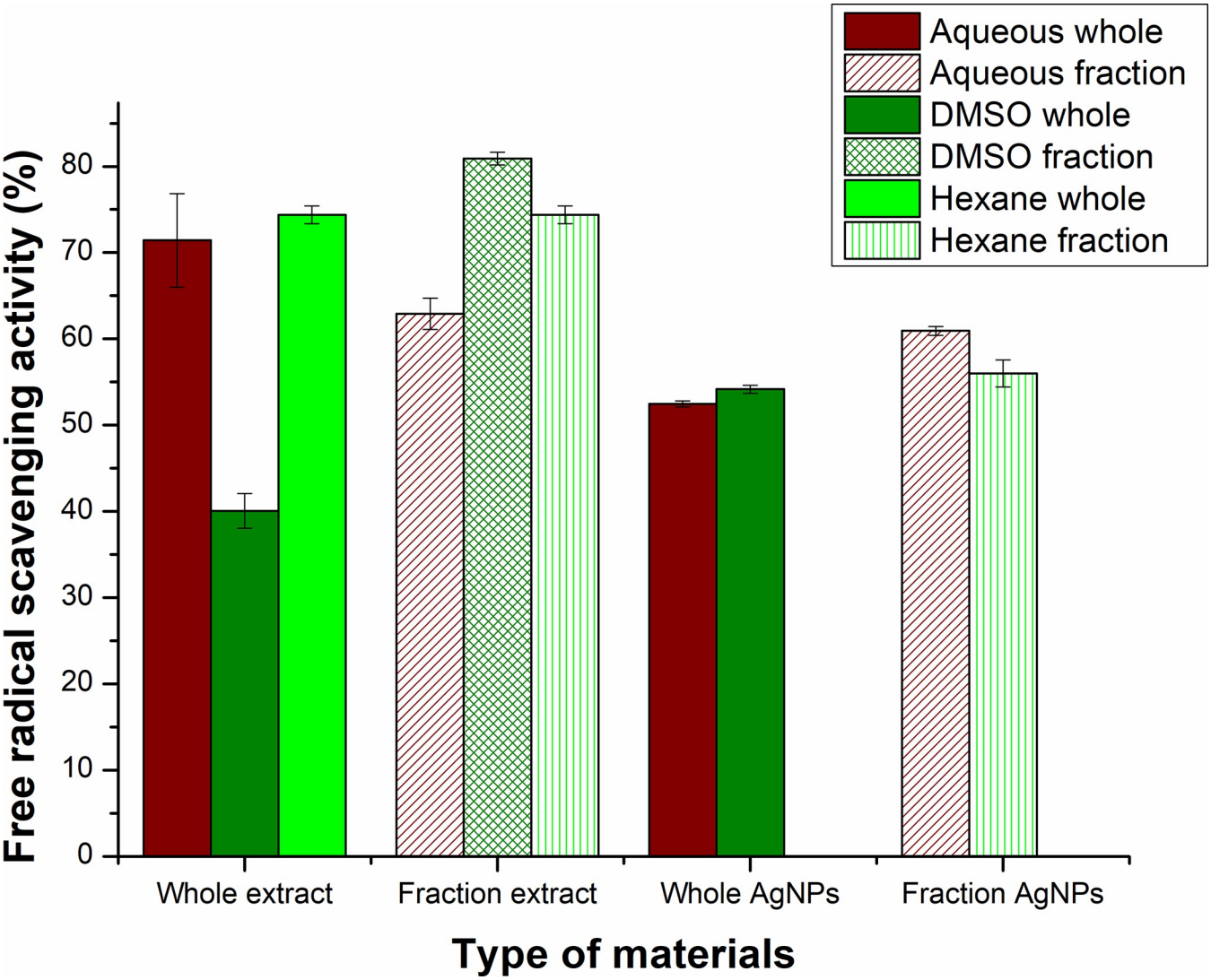


Fig 10. Antioxidant activity of plant extracts and silver nanoparticles synthesized from these extracts.

https://doi.org/10.1371/journal.pone.0287080.g010

lowest for H-extract (-3.66±0.69 mV) while Aq*-extract gave positive ORP value (67.33±0.19 mV). The given ORP values of Ag-NPs show their high oxidation potential and hence bactericidal properties. Higher positive ORP values indicate high concentration of oxidizing agents present in a solution. This corresponds to the oxidizing capability of Ag-NPs resulting in their bactericidal effects [53]. The ORP of Ag-NPs was measured to determine their oxidation potential and find their ability to oxidize bacterial cells. Among Ag-NPs the highest oxidation potential was recorded for Aq*-Ag-NPs followed by D*-Ag-NPs (Table 2). The high positive ORP value of Aq*-Ag-NPs can be linked with that of Aq*-extract. The components present in Aq*-extract that resulted in increased oxidation potential may have capped the Ag^{+} ions during biosynthesis reaction causing the formation of Aq*-Ag-NPs with high oxidizing capacity.

3.8 Identification of polyphenols through HPLC

The results of HPLC revealed the whole and fractionated extracts of S. moorcroftiana to be enriched with phenolic acids and flavonols. Such composition of the extracts make them

Table 2. Comparative analysis of Oxidation Reduction Potential of extracts and Ag-NPs synthesized from these extracts.

ORP of extracts (mV)				
Aq-extract	**Aq*-extract**	**D-extract**	**D*-extract**	**H-extract**
-113.66±2	67.33±0.33	-4.66±2.66	-65.33±1.45	-3.66±1.2
ORP of Ag-NPs (mV)				
Aq-Ag-NPs	Aq*-Ag-NPs	D-Ag-NPs	D*-Ag-NPs	H-Ag-NPs
44±0.57	110±3	70.33±2.9	92.33±4.25	-110±1.66

https://doi.org/10.1371/journal.pone.0287080.t002

efficient source for the synthesis of Ag-NPs. From the chromatogram of each of the extract, those with higher peak area (%) are picked for analysis (Table 3). Polyphenols found in Aq-extract include malic acid (25.49), caftaric acid (8.387), and myricetin (32.04). D-extract contains gallic acid (14.746), rosmarinic acid (46.227), and vitamin C (4.555). Aq*-extract possess rutin (23.884), Syringic acid (15.57), Quercitin 3,7-di-o-glucoside (47.30), and Kaempferol-3-(P-coumoryl-diglucoside)-7-glucoside (7.867) while D*-extract possess Kaempferol-3-(P-coumaroyl-diglucoside)-7-glucoside (7.867), Quercetin-3-d-galactoside (5.685), and Caffeic acid (83.03). H-extract contained the polyphenols like Gallocatechin (52.89), Gallic acid (3.230), and Kaempferol-3-feryloyl sophoroside-7-glucoside (16.00).

Plants being the natural reducing agents contain different secondary metabolites in the form of condensed polyphenols which takes part in the reduction of metal salts and stabilization of their nano forms. Identification of these secondary metabolites is vital to understand the possible reaction between the precursor and extract used [54]. Various types of polyphenols are identified in each of the extract of *S. moorcroftina*. With the help of the reaction of these phenols and flavonoids with $AgNO_3$, stable Ag-NPs in high concentration were produced. These polyphenols have been reported to possess strong antioxidant and antibacterial activity. Among the extracts, only to the D*-extract, all tested strains of bacteria were susceptible. This can also be linked to the results of TPC and TFC that show D*-extract possessing higher TFC and TPC values. Despite the presence of polyphenols in Aq and Aq*-extract, none of them showed any antibacterial activity. This is similar to the results of a study where the ethanolic extract of *Crataegus monogyna* showed good activity against Gram positive and negative bacteria while its aqueous extract did not show any. The antibacterial activity was attributed to the presence of high polyphenol content [55]. Caffeic acid is a known potent antibacterial agent which in the present study is found in high amount in D*-extract [56]. In addition, kaempferol and its derivatives have been shown in previous studies to possess good antibacterial potential against Gram positive and negative bacteria [57]. Thus, the fractionated DMSO based extract of *S. moorcroftiana* was able to extract polyphenols that were biologically active against pathogenic bacteria.

3.9 Antibacterial activity of extracts and silver nanoparticles

3.9.1 Disk diffusion assay of extracts and silver nanoparticles. The antibacterial activity of whole and fractionated *S. moorcroftiana* extracts and Ag-NPs synthesized from these extracts was examined. All types of Ag-NPs showed moderate activity against multi drug resistant human pathogens such as *Klebsiella pneumoniae*, *Pseudomonas aeruginosa*, *Staphylococcus aureus*, and *Enterococcus faecalis* (Table 4). Among the extracts, D*-extract showed good antibacterial potential with inhibition zones having diameter of 11 mm, 9.83 mm, 9.83 mm, and 10.33 mm against *K. pneumoniae*, *P. aeruginosa*, *S. aureus*, *and E. faecalis*, respectivley. The extraction of phytochemicals depends on method of extraction, solvent, and time duration. Here, solvent is considered as a main factor. On this basis, only DMSO based fraction of

Table 3. Polyphenolic compounds with their retention time and peak area (%).

Sample extract	Retention time	Compounds identity	Peak area (%)	Identification reference
Aq-extract	2.326	Malic acid	25.49	Standard
	3.209	Caftaric acid	8.387	Standard
	3.775	Gentisic acid	0.173	Standard
	24.814	Quercitin-7-o-sophoroside	0.282	Standard
	26.368	Quercitin dihydrate	0.415	Standard
	28.662	Pyrogallol	1.384	Standard
	31.152	Quercitin-3-(caffeoyl diglucoside)-7-glucoside	0.135	Standard
	34.246	Rosmarinic acid	1.222	Standard
	34.902	myricetin	32.04	Standard
D-extract	4.349	Gallic acid	14.746	Standard
	4.868	Vitamin C	46.227	Standard
	34.249	Rosmarinic acid	4.555	Standard
Aq*-extract	12.832	Morin	0.086	Standard
	14.541	P-coumaric acid	0.0717	Standard
	20.309	Quercitin-3-(caffeoyl diglucoside)-7-glucoside	2.987	Standard
	22.179	Syringic acid	15.57	Standard
	22.835	Rutin	23.884	Standard
	23.892	Quercitin 3,7-di-o-glucoside	47.30	Standard
	25.439	Kaempferol 3-(caffeoyl-diglucoside)-7-glucoside	6.779	Standard
	35.418	Kaempferol-3-feryloyl sophoroside-7-glucoside	2.368	Standard
D*-extract	18.145	Kaempferol-3-(P-coumoryl-diglucoside)-7-glucoside	7.867	Standard
	29.621	Caffeic acid	83.03	Standard
	30.44	Mandelic acid	0.337	Standard
	34.311	Rosmarinic acid	0.392	Standard
	35.741	Kaempferol-3-feryloyl sophoroside-7-glucoside	0.125	Standard

(*Continued*)

Table 3. (Continued)

Sample extract	Retention time	Compounds identity	Peak area (%)	Identification reference
H-extract	5.51	Gallocatechin	52.89	Standard
	4.25	Gallic acid	3.230	Standard
	6.358	Caffeic acid	0.309	Standard
	35.663	Kaempferol-3-feryloyl sophoroside-7-glucoside	16.00	Standard

https://doi.org/10.1371/journal.pone.0287080.t003

S. moorcroftiana rather than its aqueous extracts was able to show antibacterial effect against all the tested strains. This is probably because the plant components active against bacteria may not be effectively extracted in water while the antibacterial aromatic or saturated organic compounds are mostly obtained through organic solvent extraction [58]. As compared to D-extract, D*-extract had higher antibacterial potential. When the antibacterial activity of D*-extract is linked to the results of FTIR they indicate the presence of esters that might be responsible for its antibacterial activity because esters have been reported to possess good antibacterial activity [59]. D*-extract also possessed concentrated biological important phytochemicals such as polyphenols and flavonoids. Kumar, Nehra [60] showed that *E. faecalis* is most sensitive to plant compounds such as polyphenols. Therefore, this specific strain (as compared to other strains) in our study showed increased sensitivity to H-extract, D-extract, and D*-extract.

The largest zone of inhibition was 12 mm that was recorded for Aq-Ag-NPs against *K. pneumoniae* and D*-Ag-NPs against *P. aeruginosa*. When compared, Aq-Ag-NPs gave larger zone of inhibition than Aq*-Ag-NPs but in case of DMSO extract based Ag-NPs, D*-Ag-NPs showed higher antibacterial activity than D-Ag-NPs. H-Ag-NPs gave comparatively smaller zones of inhibition i.e. 8 mm, 9.33 mm, 8.67 mm, and 8.60 mm against *K. pneumoniae*, *P. aeruginosa*, *S. aureus*, *and E. faecalis*, respectivley, revealing it to be weak antibacterial agent. Four types of controls were taken alongside i.e. dH_2O, DMSO, hexane, and ceftadizime antibiotic (200μg/ml).

Each type of Ag-NPs showed activity against all tested MDR strains. H-Ag-NPs were the least effective because H-extract did not contain enough phytochemicals to synthesize and cap Ag-NPs. As in our results we can see that D*-Ag-NPs are more stable, have higher antioxidant activity, contain increased amount of phenolic and flavonoid compounds, and also have the high oxidation potential which should how make them most effective against resistant bacteria. However, Aq-Ag-NPs were the most effective with large inhibition zone against each bacterium as compared to all other Ag-NPs. The antibacterial results linked with FTIR analysis revealed the presence of S = O (sulfoxide) on Aq-Ag-NPs that is commonly found in organosulfur compounds having strong antibacterial activity along with other phytochemicals [61]. For instance, thiosulfinate (organosulfur compound) such as allicin has been recognized as

Table 4. Inhibition zone sizes of Ag-NPs against MDR bacteria.

Bacterial strains	Zone of inhibition (mm)									
	H-Ag-NPs	Aq*-Ag-NPs	D*-Ag-NPs	Aq-Ag-NPs	D-Ag-NPs	H-extract	Aq*-extract	D*-extract	Aq-extract	D-extract
Klebsiella pneumonia	8±0	11±0	11±0	12±0	11±0	0	0	11±0	0	0
Pseudomonas aeruginosa	9.33±0.33	10.33±0.33	12	11.66±0.33	9.33±0.33	0	0	9.83±0.44	0	0
Staphylococcus aureus	8.67±0.33	10.66±0.33	10.5±0.28	11±0	9.83±0.16	0	0	9.83±0.44	0	0
Enterococcus faecalis	8.60±0.16	10±0	11.33±0.33	11.5±0.28	11±0.57	11.3±0	0	10.33±0.33	0	10±0

https://doi.org/10.1371/journal.pone.0287080.t004

Table 5. Minimum inhibitory concentration of Ag-NPs against resistant pathogenic strain.

Bacterial strains	Minimum inhibitory concentration (μg/mL)				
	H-Ag-NPs	Aq*-Ag-NPs	D*-Ag-NPs	Aq-Ag-NPs	D-Ag-NPs
Klebsiella pneumonia	250	125	62.5	15.625	62.5
Pseudomonas aeruginosa	7.8	31.25	31.25	7.8	31.25
Staphylococcus aureus	500	31.25	62.5	31.25	125
Enterococcus faecalis	500	250	31.25	15.625	62.5

https://doi.org/10.1371/journal.pone.0287080.t005

responsible for the antibacterial property of garlic and onion [62]. The contributing role of these compounds with other phytochemicals may be the reason for enhanced antibacterial activity of Aq-Ag-NPs. Though the same group was also found in Aq*-Ag-NPs, their antibacterial potential was not that effective because at the end of fractionation (solvent-solvent extraction), water had few remaining phytochemicals to extract and further utilize for synthesis and capping of Ag-NPs. Such organosulfur compounds are immiscible in water and are often more soluble in less polar solvents than water [42,63]. Therefore, these compounds were not biologically available in Aq-extract and Aq*-extract for interaction with bacteria, hence did not show any antibacterial activity.

3.9.2 Minimum Inhibitory concentration (MIC) of Ag-NPs. The minimum inhibitory concentrations of Ag-NPs against all aforementioed bacterial strains were determined through microdilution assay. The bacterial growth inhibition with the application of Ag-NPs was determined through visual observation of turbidity in the wells of microtitre plate. Each kind of Ag-NPs showed different MIC values against each bacterial strain as shown in Table 5. The lowest MIC of various Ag-NPs against the given bacterial strains are: 7.8 μg/mL of H-Ag-NPs against *P. aeruginosa*, 31.25 μg/mL of Aq*-Ag-NPs against *P. aeruginosa* and *Staphylococcus aureus*, 31.25 μg/mL of D*-Ag-NPs against *P. aeruginosa* and *E. faecalis*, 7.8 μg/mL of Aq-Ag-NPs against *P. aeruginosa*, and 31.25 μg/mL of D-Ag-NPs against *P. aeruginosa*. Thus, from these results, it is clear that *P. aeruginosa* is the most sensitive to all kinds of Ag-NPs even at very low concentrations. Similar results were shown by de Lacerda Coriolano, de Souza [64] where *P. aeruginosa* was sensitive to the concentrations of Ag-NPs between 1 and 200 μg/mL. All types of Ag-NPs were effective in their lower concentrations that ultimately reduce their cytotoxic effects. However, like the results of disk diffusion assay, Aq-Ag-NPs against each bacterium compared to other Ag-NPs revealed to be relatively effective in lower concentrations such as 15.625 μg/mL, 7.8 μg/mL, 31.25 μg/mL, and 15.625 μg/mL against *K. pneumoniae*, *P. aeruginosa*, *S. aureus*, and *E. faecalis*, respectively.

3.9.3. Demonstration of the mechanism of action of bacterial inhibition by Ag-NPs. One of the main mechanisms through which antimicrobials induce bactericidal effect is the

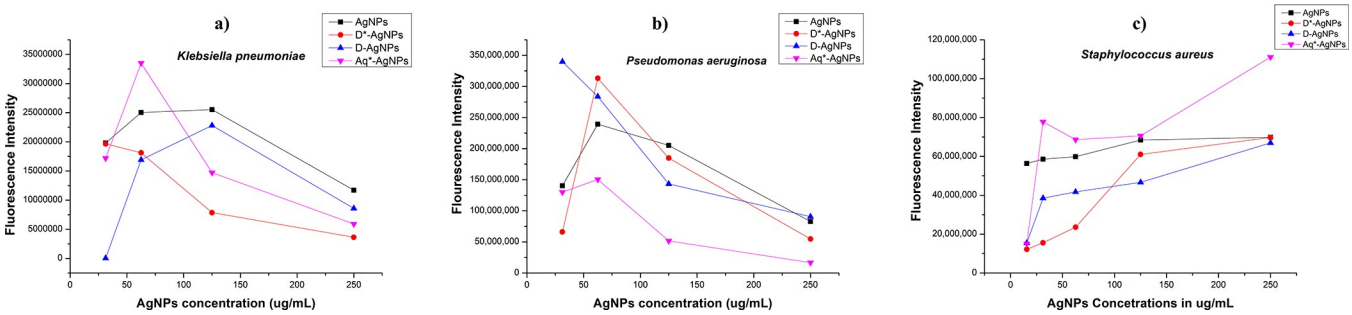


Fig 11. Reactive oxygen quantification in bacterial cultures grown in the presence of different concentrations of different types of Ag-NPs.

https://doi.org/10.1371/journal.pone.0287080.g011

generation of reactive oxygen species. These ROS targets and alter the sites of amino acids and nucleotides, resulting in protein and DNA damage, causing bacterial cell death [65]. The results of ROS quantification shows the production of ROS in all three types of bacteria by all types of applied Ag-NPs (Fig 11). The highest level of ROS was generated varyingly in each of the bacterial culture, such as, Aq*-Ag-NPs was able to produce increased level of ROS in *K. pneumonia* and *S. aureus*, while in *P. aeruginosa*, D*-Ag-NPs produced increased level of ROS. Also, in each bacterial culture, Aq-Ag-NPs consistently generated significant amount of ROS. A similar trend with respect to the relation of concentration of Ag-NPs and fluorescence intensity of ROS was noted in *K. pneumoniae* and *P. aeruginosa*. In these bacterial cultures at low concentrations of Ag-NPs (31.2–62.5 μg/mL), the ROS are generated in high numbers, but as soon as the concentration of Ag-NPs increases (reaches 250 μg/mL), the number of ROS falls gradually. This might occur because with the application of higher concentrations of Ag-NPs the bacterial cells die and ultimately they are not able to produce ROS [66]. However, in *S. aureus*, the number of ROS retained to increase with increase in the concentration of Ag-NPs. Thus, all Ag-NPs were shown to be applicable as antibacterial agents because of their reasonably high inhibitive activity even in very less concentrations.

4. Conclusion

Green synthesized Ag-NPs because of their ecofriendly synthesis and enhanced antibacterial activity have gained enormous attention of researchers to provide solution for antibiotic resistance. In this study, the extract of *S. moorcroftiana* (whole and fraction) was used for the synthesis of Ag-NPs in three solvents (water, DMSO, and hexane) with decreasing polarity. The characterization techniques confirmed the synthesis of spherical Ag-NPs in high concentration with average diameter less than 20 nm, having high polydispersity and stability. Phytochemicals like proteins, flavonoids, phenolic compounds and organic acids are identified to be significantly involved in the synthesis of Ag-NPs. These compounds, when extracted in fractions show their targeted role in the synthesis of Ag-NPs and their antibacterial effect, as observed in D*-extract. The plant compounds extracted in DMSO after extraction through hexane showed good reducing, stabilizing, and antibacterial potential. Regardless of identifying the targeted role of phytochemicals, Aq-Ag-NPs were found to be most effective antibacterial agents because of diverse phytochemicals (wholly extracted in water) capped on them. Overall, this study showed that the targeted extraction of phytochemicals from medicinal plant like *S. moorcroftiana* can help to obtain the antimicrobial plant components that can be applied against bacteria and used for the synthesis of Ag-NPs with enhanced antibacterial activity and reduced toxicity.

Acknowledgments

The authors acknowledge the role of the University of Malakand, Pakistan for the required funding in providing a conducive environment for research activities. The authors acknowledge the role of the Centralized Resource Laboratory, University of Peshawar, Pakistan and Department of Chemistry, Comsats University Abbottabad Pakistan for providing analytical facilities. The authors also acknowledge the role of the international foundation for Science in Sweden. Tauqir A. Sherazi acknowledges the financial support from the Alexander von Humboldt Foundation.

Author Contributions

Conceptualization: Tariq Khan.

Data curation: Maham Khan.

Formal analysis: Shahid Wahab, Tauqir A. Sherazi.

Funding acquisition: Tariq Khan.

Investigation: Muhammad Zahoor.

Methodology: Muhammad Zahoor.

Project administration: Tariq Khan.

Resources: Tariq Khan.

Software: Muhammad Aasim, Tauqir A. Sherazi.

Supervision: Tariq Khan.

Validation: Muhammad Aasim.

Visualization: Maham Khan, Shahid Wahab.

Writing – original draft: Maham Khan.

Writing – review & editing: Tariq Khan, Soon-Il Yun.

References

1. Slavin YN, Ivanova K, Hoyo J, Perelshtein I, Owen G, Haegert A, et al. Novel lignin-capped silver nanoparticles against multidrug-resistant bacteria. ACS Applied Materials and Interfaces. 2021; 13 (19):22098–109. https://doi.org/10.1021/acsami.0c16921 PMID: 33945683
2. Qais FA, Shafiq A, Khan HM, Husain FM, Khan RA, Alenazi B, et al. Antibacterial effect of silver nanoparticles synthesized using Murraya koenigii (L.) against multidrug-resistant pathogens. Bioinorganic Chemistry and Applications. 2019;2019. https://doi.org/10.1155/2019/4649506 PMID: 31354799
3. Das CA, Kumar VG, Dhas TS, Karthick V, Govindaraju K, Joselin JM, et al. Antibacterial activity of silver nanoparticles (biosynthesis): A short review on recent advances. Biocatalysis Agricultural Biotechnology. 2020; 27:101593.
4. Tang S, Zheng J. Antibacterial activity of silver nanoparticles: structural effects. Advanced Healthcare Materials. 2018; 7(13):1701503. https://doi.org/10.1002/adhm.201701503 PMID: 29808627
5. Franci G, Falanga A, Galdiero S, Palomba L, Rai M, Morelli G, et al. Silver nanoparticles as potential antibacterial agents. Molecules 2015; 20(5):8856–74. https://doi.org/10.3390/molecules20058856 PMID: 25993417
6. Lee W, Kim K-J, Lee DGJB. A novel mechanism for the antibacterial effect of silver nanoparticles on Escherichia coli. 2014; 27(6):1191–201.
7. Buszewski B, Rogowska A, Railean-Plugaru V, Złoch M, Walczak-Skierska J, Pomastowski PJM. The influence of different forms of silver on selected pathogenic bacteria. 2020; 13(10):2403.
8. Lu J, Wang Y, Jin M, Yuan Z, Bond P, Guo JJWr. Both silver ions and silver nanoparticles facilitate the horizontal transfer of plasmid-mediated antibiotic resistance genes. 2020; 169:115229.
9. Khojasteh-Taheri R, Ghasemi A, Meshkat Z, Sabouri Z, Mohtashami M, Darroudi M, et al. Green synthesis of silver nanoparticles using Salvadora persica and Caccinia macranthera extracts: Cytotoxicity analysis and antimicrobial activity against antibiotic-resistant bacteria. Applied Biochemistry. 2023:1–16. https://doi.org/10.1007/s12010-023-04407-y PMID: 36847984
10. Ahmad S, Munir S, Zeb N, Ullah A, Khan B, Ali J, et al. Green nanotechnology: A review on green synthesis of silver nanoparticles—An ecofriendly approach. International Journal of Nanomedicine. 2019; 14:5087. https://doi.org/10.2147/IJN.S200254 PMID: 31371949
11. Rafique M, Sadaf I, Rafique MS, Tahir MB. A review on green synthesis of silver nanoparticles and their applications. Artificial cells, Nanomedicine, and Biotechnology. 2017; 45(7):1272–91.
12. Srikar SK, Giri DD, Pal DB, Mishra PK, Upadhyay SN. Green synthesis of silver nanoparticles: a review. Green and Sustainable Chemistry. 2016; 6(1):34–56.
13. Oves M, Rauf MA, Aslam M, Qari HA, Sonbol H, Ahmad I, et al. Green synthesis of silver nanoparticles by Conocarpus Lancifolius plant extract and their antimicrobial and anticancer activities. Saudi Journal

of Biological Sciences. 2022; 29(1):460–71. https://doi.org/10.1016/j.sjbs.2021.09.007 PMID: 35002442

14. Farshori NN, Al-Oqail MM, Al-Sheddi ES, Al-Massarani SM, Saquib Q, Siddiqui MA, et al. Green synthesis of silver nanoparticles using Phoenix dactylifera seed extract and its anticancer effect against human lung adenocarcinoma cells. Journal of Drug Delivery Science Technology. 2022; 70:103260.
15. Swamy VS, Prasad R. Green synthesis of silver nanoparticles from the leaf extract of Santalum album and its antimicrobial activity. Optoelectronic and Biomedical Materials. 2012; 4(3):53–9.
16. Baghani M, Es-haghi A. Characterization of silver nanoparticles biosynthesized using Amaranthus cruentus. Bioinspired, Biomimetic and Nanobiomaterials. 2019; 9(3):129–36.
17. Ghaffari-Moghaddam M, Hadi-Dabanlou R, Khajeh M, Rakhshanipour M, Shameli K. Green synthesis of silver nanoparticles using plant extracts. Korean Journal of Chemical Engineering. 2014; 31(4):548–57.
18. Sultana B, Anwar F, Ashraf M. Effect of extraction solvent/technique on the antioxidant activity of selected medicinal plant extracts. Molecules. 2009; 14(6):2167–80. https://doi.org/10.3390/molecules14062167 PMID: 19553890
19. Dhawan D, Gupta JJIJBC. Research article comparison of different solvents for phytochemical extraction potential from datura metel plant leaves. International Journal of Biological Chemistry. 2017; 11 (1):17–22.
20. Rokosz P, Stachowicz K, Kwiecień HJNpr. Phytochemical analysis of non-polar solvent extracts of the *Wisteria sinensis* leaves. Natural product research. 2018; 32(20):2487–9.
21. Irfan M, Qadir MIJPJPS. Analgesic, anti-inflammatory and antipyretic activity of Salvia moorcroftiana. Pakistan Journal of Pharmaceutical Science. 2017; 30(2):481–6.
22. Wahid F, Jan T, Al-Joufi FA, Ali Shah SW, Nisar M, Zahoor M. Amelioration of scopolamine-induced cognitive dysfunction in experimental mice using the medicinal plant Salvia moorcroftiana. Brain Sciences. 2022; 12(7):894. https://doi.org/10.3390/brainsci12070894 PMID: 35884701
23. Gani R, Bhat ZA, Dar MA, Shah Z. Pharmacognostic and phytochemical characteristics of the aerial part of Salvia moorcroftiana wall. Ex Benth. Growing wild in Kashmir Valley, India. Pharmaceutical Methods 2019; 10(1):3–47.
24. Mehmood A, Javid S, Khan MF, Ahmad KS, Mustafa A. In vitro total phenolics, total flavonoids, antioxidant and antibacterial activities of selected medicinal plants using different solvent systems. BMC Chemistry. 2022; 16(1):1–10.
25. Beigoli S, Sabouri Z, Moghaddas SSTH, Heydari A, Darroudi M. Exploring the biophysical properties, synergistic antibacterial activity, and cell viability of nanocomposites containing casein phosphopeptides and amorphous calcium phosphate. Journal of Drug Delivery Science Technology. 2023:104680.
26. Zuas O, Hamim N, Sampora Y. Bio-synthesis of silver nanoparticles using water extract of Myrmecodia pendan (Sarang Semut plant). Materials Letters. 2014; 123:156–9.
27. Mehata MS. Green route synthesis of silver nanoparticles using plants/ginger extracts with enhanced surface plasmon resonance and degradation of textile dye. Materials Science Engineering: B. 2021; 273:115418.
28. Parekh J, Jadeja D, Chanda S. Efficacy of aqueous and methanol extracts of some medicinal plants for potential antibacterial activity. Turkish Journal of Biology. 2005; 29(4):203–10.
29. Ashraf JM, Ansari MA, Khan HM, Alzohairy MA, Choi I. Green synthesis of silver nanoparticles and characterization of their inhibitory effects on AGEs formation using biophysical techniques. Scientific reports. 2016; 6(1):1–10.
30. Isa N, Osman MS, Abdul Hamid H, Inderan V, Lockman Z. Studies of surface plasmon resonance of silver nanoparticles reduced by aqueous extract of shortleaf spikesedge and their catalytic activity. International journal of phytoremediation. 2023; 25(5):658–69. https://doi.org/10.1080/15226514.2022.2099345 PMID: 35858487
31. Bar H, Bhui DK, Sahoo GP, Sarkar P, De SP, Misra A. Green synthesis of silver nanoparticles using latex of Jatropha curcas. Colloids surfaces A: Physicochemical engineering aspects. 2009; 339(1–3):134–9.
32. Doak J, Gupta R, Manivannan K, Ghosh K, Kahol PK. Effect of particle size distributions on absorbance spectra of gold nanoparticles. Physica E: Low-dimensional Systems Nanostructures. 2010; 42 (5):1605–9.
33. Kochkina NEe, Skobeleva O. Synthesis of silver nanoparticles in DMSO solutions of starch: a comparative investigation of native and soluble starches. Наносистемы: физика, химия, математика. 2015; 6 (3):405–11.
34. Ramazanli V, Ahmadov I. Synthesis of silver nanoparticles by using extract of olive leaves. Adv Biol Earth Sci. 2022; 7(3):238–44.

35. Ahmed S, Saifullah, Ahmad M, Swami BL, Ikram S, sciences a. Green synthesis of silver nanoparticles using Azadirachta indica aqueous leaf extract. Journal of radiation research. 2016; 9(1):1–7.

36. Felhi S, Daoud A, Hajlaoui H, Mnafgui K, Gharsallah N, Kadri A. Solvent extraction effects on phytochemical constituents profiles, antioxidant and antimicrobial activities and functional group analysis of Ecballium elaterium seeds and peels fruits. Food Science Technology. 2017; 37:483–92.

37. Padi PM, Adetunji TL, Unuofin JO, Mchunu CN, Ntuli NR, Siebert F. Phytochemical, antioxidant, and functional group analyses of South African Evolvulus alsinoides (L.) L. South African Journal of Botany. 2022; 149:170–7.

38. Aslam M, Fozia F, Gul A, Ahmad I, Ullah R, Bari A, et al. Phyto-Extract-Mediated Synthesis of Silver Nanoparticles Using Aqueous Extract of Sanvitalia procumbens, and Characterization, Optimization and Photocatalytic Degradation of Azo Dyes Orange G and Direct Blue-15. Molecules. 2021; 26 (20):6144. https://doi.org/10.3390/molecules26206144 PMID: 34684724

39. Majoumouo MS, Sibuyi NRS, Tincho MB, Mbekou M, Boyom FF, Meyer M. Enhanced anti-bacterial activity of biogenic silver nanoparticles synthesized from Terminalia mantaly Extracts. International Journal of Nanomedicine. 2019; 14:9031. https://doi.org/10.2147/IJN.S223447 PMID: 31819417

40. Sbihi HM, Nehdi IA, Mokbli S, Romdhani-Younes M, Al-Resayes SI. Hexane and ethanol extracted seed oils and leaf essential compositions from two castor plant (Ricinus communis L.) varieties. Industrial Crops Products. 2018; 122:174–81.

41. Kyung KH. Antimicrobial activity of volatile sulfur compounds in foods. Volatile Sulfur Compounds in Food: ACS Publications; 2011. p. 323–38.

42. Leontiev R, Hohaus N, Jacob C, Gruhlke MC, Slusarenko AJ. A comparison of the antibacterial and antifungal activities of thiosulfinate analogues of allicin. Scientific Reports. 2018; 8(1):1–19.

43. Rauwel P, Küünal S, Ferdov S, Rauwel E. A review on the green synthesis of silver nanoparticles and their morphologies studied via TEM. Advances in Materials Science Engineering. 2015;2015.

44. Hedberg J, Lundin M, Lowe T, Blomberg E, Wold S, Wallinder IO. Interactions between surfactants and silver nanoparticles of varying charge. Journal of Colloid and Interface Science. 2012; 369(1):193–201. https://doi.org/10.1016/j.jcis.2011.12.004 PMID: 22204969

45. Rao YS, Kotakadi VS, Prasad T, Reddy AV, Gopal DS. Green synthesis and spectral characterization of silver nanoparticles from Lakshmi tulasi (Ocimum sanctum) leaf extract. Spectrochimica Acta Part A: Molecular Biomolecular Spectroscopy. 2013; 103:156–9.

46. Jang M-H, Lee S, Hwang YS. Characterization of silver nanoparticles under environmentally relevant conditions using asymmetrical flow field-flow fractionation (AF4). Plos One. 2015; 10(11):e0143149. https://doi.org/10.1371/journal.pone.0143149 PMID: 26575993

47. Alahmad A, Feldhoff A, Bigall NC, Rusch P, Scheper T, Walter J-G. Hypericum perforatum L.-mediated green synthesis of silver nanoparticles exhibiting antioxidant and anticancer activities. Nanomaterials. 2021; 11(2):487. https://doi.org/10.3390/nano11020487 PMID: 33673018

48. Čuk N, Šala M, Gorjanc M. Development of antibacterial and UV protective cotton fabrics using plant food waste and alien invasive plant extracts as reducing agents for the in-situ synthesis of silver nanoparticles. Cellulose. 2021; 28(5):3215–33.

49. Mohamad NAN, Arham NA, Jai J, Hadi A. Plant extract as reducing agent in synthesis of metallic nanoparticles: a review. Advanced Materials Research. 2014; 832:350–5.

50. Khan ZUH, Khan A, Chen YM, Shah NS, Khan AU, Muhammad N, et al. Enhanced antimicrobial, antioxidant applications of green synthesized Ag-NPs-an acute chronic toxicity study of phenolic azo dyes & study of materials surface using X-ray photoelectron spectroscopy. Journal of Photochemistry Photobiology B: Biology. 2018; 180:208–17.

51. Mat Yusuf SNA, Che Mood CNA, Ahmad NH, Sandai D, Lee CK, Lim V. Optimization of biogenic synthesis of silver nanoparticles from flavonoid-rich Clinacanthus nutans leaf and stem aqueous extracts. Royal Society Open Science. 2020; 7(7):200065. https://doi.org/10.1098/rsos.200065 PMID: 32874618

52. Demir S, Turan I, Aliyazicioglu Y. Selective cytotoxic effect of Rhododendron luteum extract on human colon and liver cancer cells. BUON. 2016; 21(4):883–8. PMID: 27685909

53. Ahuja S. Evaluating water quality to prevent future disasters: Academic Press; 2019.

54. Anand KKH, Mandal BK. Activity study of biogenic spherical silver nanoparticles towards microbes and oxidants. Spectrochimica Acta Part A: Molecular Biomolecular Spectroscopy. 2015; 135:639–45.

55. Ignat I, Radu DG, Volf I, Pag AI, Popa VI. Antioxidant and antibacterial activities of some natural polyphenols. cytokines. 2013; 4:387–99.

56. Kępa M, Miklasińska-Majdanik M, Wojtyczka RD, Idzik D, Korzeniowski K, Smoleń-Dzirba J, et al. Antimicrobial potential of caffeic acid against Staphylococcus aureus clinical strains. BioMed research international. 2018;2018. https://doi.org/10.1155/2018/7413504 PMID: 30105241

57. Periferakis A, Periferakis K, Badarau IA, Petran EM, Popa DC, Caruntu A, et al. Kaempferol: Antimicrobial Properties, Sources, Clinical, and Traditional Applications. International Journal of Molecular Sciences. 2022; 23(23):15054. https://doi.org/10.3390/ijms232315054 PMID: 36499380

58. Jain I, Jain P, Bisht D, Sharma A, Srivastava B, Gupta N. Comparative evaluation of antibacterial efficacy of six Indian plant extracts against Streptococcus mutans. Journal of clinical diagnostic research: JCDR. 2015;9(2):ZC50. https://doi.org/10.7860/JCDR/2015/11526.5599 PMID: 25859526

59. Shaaban MT, Ghaly MF, Fahmi SM. Antibacterial activities of hexadecanoic acid methyl ester and green-synthesized silver nanoparticles against multidrug-resistant bacteria. Journal of basic microbiology. 2021; 61(6):557–68. https://doi.org/10.1002/jobm.202100061 PMID: 33871873

60. Kumar M, Nehra K, Duhan J. Phytochemical analysis and antimicrobial efficacy of leaf extracts of Pithecellobium dulce. Asian Journal of Pharmaceutical Clinical Research. 2013; 6(1):70–6.

61. Bhatwalkar SB, Mondal R, Krishna SBN, Adam JK, Govender P, Anupam RFiM. antibacterial properties of organosulfur compounds of garlic (Allium sativum). Frontiers in Microbiology. 2021;12. https://doi.org/10.3389/fmicb.2021.613077 PMID: 34394014

62. Patra AK. An overview of antimicrobial properties of different classes of phytochemicals. Dietary Phytochemicals and Microbes. 2012:1–32.

63. Haminiuk CWI, Plata-Oviedo MSV, de Mattos G, Carpes ST, Branco IG. Extraction and quantification of phenolic acids and flavonols from Eugenia pyriformis using different solvents. Journal of Food Science Technology 2014; 51(10):2862–6. https://doi.org/10.1007/s13197-012-0759-z PMID: 25328239

64. de Lacerda Coriolano D, de Souza JB, Bueno EV, Medeiros SMdFRdS, Cavalcanti IDL, Cavalcanti IMF. Antibacterial and antibiofilm potential of silver nanoparticles against antibiotic-sensitive and multidrug-resistant Pseudomonas aeruginosa strains. Brazilian Journal of Microbiology. 2021; 52(1):267–78.

65. Tripathi R, Gupta R, Sahu M, Srivastava D, Das A, Ambasta RK, et al. Free radical biology in neurological manifestations: mechanisms to therapeutics interventions. Environmental Science Pollution Research. 2021:1–48. https://doi.org/10.1007/s11356-021-16693-2 PMID: 34617231

66. Khan T, Ali GS. Variation in surface properties, metabolic capping, and antibacterial activity of biosynthesized silver nanoparticles: comparison of bio-fabrication potential in phytohormone-regulated cell cultures and naturally grown plants. RSC advances. 2020; 10(64):38831–40. https://doi.org/10.1039/d0ra08419k PMID: 35518444